3D MICROFABRICATION OF BIOLOGICAL MACHINES

BY

RITU RAMAN

THESIS

Submitted in partial fulfillment of the requirements
for the degree of Master of Science in Mechanical Engineering
in the Graduate College of the
University of Illinois at Urbana-Champaign, 2013

Urbana, Illinois

Advisers:

Professor Rashid Bashir
Professor Taher Saif

ABSTRACT

The burgeoning field of additive manufacturing, or "3D printing", centers on the idea of creating three-dimensional objects from digital models. While conventional manufacturing approaches rely on modifying a base material via subtractive processes such as drilling or cutting, 3D printing creates three-dimensional objects through successive deposition of two-dimensional layers. By enabling rapid fabrication of complex objects, 3D printing is revolutionizing the fields of engineering design and manufacturing. This thesis details the development of a projection-based stereolithographic 3D printing apparatus capable of high-resolution patterning of living cells and cell signals dispersed in an absorbent hydrogel polymer matrix *in vitro*. This novel enabling technology can be used to create model cellular systems that lead to a quantitative understanding of the way cells sense, process, and respond to signals in their environment.

The ability to pattern cells and instructive biomaterials into complex 3D patterns has many applications in the field of tissue engineering, or "reverse engineering" of cellular systems that replicate the structure and function of native tissue. While the goal of reverse engineering native tissue is promising for medical applications, this idea of building with biological components concurrently brings about a new discipline: "forward engineering" of biological machines and systems. In addition to rebuilding existing systems with cells, this technology enables the design and forward engineering of novel systems that harness the innate dynamic abilities of cells to self-organize, self-heal, and self-replicate in response to environmental cues. This thesis details the development of skeletal and cardiac muscle based bioactuators that can sense external electrical and optical signals and demonstrate controlled locomotive behavior in response to them. Such machines, which can sense, process, and respond to signals in a dynamic environment, have a myriad array of applications including toxin neutralization and high throughput drug testing *in vitro* and drug delivery and programmable tissue engineered implants *in vivo*.

A synthesis of two fields, 3D printing and tissue engineering, has brought about a new discipline: using microfabrication technologies to forward engineer biological machines and systems capable of complex functional behavior. By introducing a new set of "building blocks" into the engineer's toolbox, this new era of design and manufacturing promises to open up a field of research that will redefine our world.

ACKNOWLEDGEMENTS

I dedicate this thesis to my mother, Radha Raman, my father, Raman Radhakrishnan, and my grandfather, K.R. Dorairaj – the three engineers that have inspired me throughout my life.

Thank you, Professor Rashid Bashir, for your invaluable advice and support throughout my graduate school career. Joining your lab has opened up an amazing array of opportunities and I am really looking forward to continuing my doctoral research with you.

Thank you, Professor Taher Saif, for your help in understanding the mechanical behavior of biological machines.

Thank you, Dr. Vincent Chan, for your mentorship, guidance, and friendship. I am truly grateful for everything you have taught me and will always be inspired by your passion for research.

Thank you, Caroline Cvetkovic, for your mentorship and collaboration on these experiments. I'm so glad that we can work together as a team throughout graduate school.

Thank you Dr. Mustafa Mir, Dr. Basanta Bhaduri, and Professor Gabriel Popescu for helping me design and build the micro-stereolithography apparatus.

Thank you to Dr. Michael Poellman, Dr. Piyush Bajaj, Dr. Mayandi Sivaguru, Dr. Larry Millet, Brian Williams, Michael Grigola, Samir Mishra, Madeline Tolish, and Stephanie Nemec for assisting me on various aspects of these projects.

Thank you Devin Neal, Sebastien Uzel, Dr. Mahmut Selman Sakar, Professor Hyun Joon Kong, Professor Harry Asada, and Professor Roger Kamm for your helpful advice and discussions in planning this research.

I am grateful for the National Science Foundation Integrative Graduate Education and Research Traineeship that has funded my graduate education and research in cellular mechanics and bionanotechnology (CMMB IGERT, Grant 0965918). I am also grateful for the funding for my research in engineered biological machines provided by the National Science Foundation Science and Technology Center (EBICS, Grant 0939511).

Finally, I would like to thank my parents for inspiring me to dream big and become a socially responsible engineer and inventor. You are my motivation to work hard and succeed. A special thank you to my two best friends, Abhinav Rao and Sasha Patkin, for helping me laugh my way through graduate school. Thank you to all the new friends I have made at the University of Illinois, I am so glad to know you and look forward to the years of study we have ahead of us!

TABLE OF CONTENTS

CHAPTER 1: INTRODUCTION

1.1 MOTIVATION

The advent of 3D printing additive manufacturing technologies has revolutionized engineering design and manufacturing in recent years. The use of these technologies to manufacture products with traditional engineering materials such as metals and plastics is being extensively explored and promises to permeate through all aspects of industry. The concurrent rise of tissue engineering, a new era of biological and biomedical engineering, has given rise to the concept of "building with biology". This field is centered on the idea that scientists and engineers can combine cells and instructive biomaterials to fabricate complex biological substitutes for native tissue and organs. This thesis presents a synthesis of these two rapidly evolving fields: using 3D printing technology to microfabricate biological machines and systems capable of complex sensing and actuation behaviors.

1.2 OVERVIEW

This thesis presents the development of a high-resolution stereolithographic 3D printing apparatus designed to replicate complex cellular microenvironments, followed by a demonstration of microfabricated skeletal and cardiac muscle based biological machines controlled via external electrical and optical signaling.

Chapter 2 begins with a literature review of stereolithographic 3D printing processes and their applications in engineering 3D cell culture systems. This is followed by a review of "reverse-engineered" biological systems for applications in tissue engineering and regenerative medicine, and then a review of "forward-engineered" biological systems for applications in biosensing and bioactuation.

Chapter 3 outlines the development of a projection stereolithography-based 3D printing system that is capable of printing cells and instructive biomaterials at high resolution.

Chapter 4 presents forward-engineered biological machines powered by the actuation of engineered skeletal and cardiac muscle.

Chapter 5 describes future directions in the new field of microfabricating biological machines and systems, followed by a discussion on novel applications of this technology.

CHAPTER 2: REVIEW OF ENGINEERED BIOLOGICAL SYSTEMS

2.1 MICROFABRICATION OF BIOLOGICAL SYSTEMS

2.1.1 CELL INTERACTIONS WITH 3D MATRICES

Cells in native tissue are arranged in complex three-dimensional structures and surrounded by a range of biological, chemical, and mechanical signals that are specifically tuned to evoke certain functional responses. The boundary conditions imposed by the highly structured microenvironment of cells in live tissues and organs affect cell architecture and function (Watt 2013). Indeed, it has been shown that cellular phenotype can even supersede genotype as a result of interaction with the extra-cellular matrix (ECM) that surrounds cells *in vivo* (Petersen 1992).

Conventionally, cells cultured in monolayers upon stiff flat substrates such as plastic or glass petri dishes have served as representative models of the functional behavior of native tissue. These models have provided researchers with much insight into many biological phenomena. Pioneering studies on the effect of 2D substrate stiffness on the directed differentiation of plated stem cells (Engler 2006) and the mechanical interactions that lead to changes in cell growth and apoptosis (Chen 1997) have contributed greatly to the field's understanding of the functional behavior of a cell.

However, it is well recognized that the range of complex signaling mechanisms and three-dimensional cell-cell and cell-matrix interactions found in real tissue cannot be replicated by these two-dimensional models (Pampaloni 2007). In fact, studies of cells embedded in 3D matrices have been shown to demonstrate significantly different functional behavior than present in the conventional 2D case (Fraley 2010). Studying the 3D communication network regulating cell-matrix interactions in native tissue can thus lead to an improved understanding of the physiological mechanisms underlying cell growth, proliferation, migration, differentiation and even tissue organization and remodeling on the macro-scale (Cukierman 2002).

Experimental studies of three-dimensional morphology and phenomena in cellular systems have primarily been conducted in live animals, but there are many limitations on the experimental flexibility allowed in such *in vivo* studies. The challenging task of reliable imaging

and data collection inside live animals, for example, renders these experiments difficult to characterize and indicates the need for an alternative approach to studying cells in 3D models.

The underlying challenge in this field is, therefore, to fabricate 3D *in vitro* cell culture systems that can mimic the morphology and functional behavior of native tissues better than conventional 2D monolayer cultures. This promises to provide a quantitative understanding of the mechanisms underlying the way cells sense, process, and respond to signals in their environment. Such systems have applications in fundamental studies of extracellular matrix interactions (Thery 2010), organ-on-a-chip methods for drug screening of physiologically and phenotypically relevant substitutes for native tissue (Huh 2010), programmable tissue engineering for applications regenerative medicine (Andersson 2004), and the development of biological sensors and actuators (Kamm 2013). All these applications require an enabling microfabrication technology that is capable of patterning cells and cell signals at high resolution in a 3D environment.

2.1.2 STEREOLITHOGRAPHIC 3D PRINTING

An array of rapid prototyping technologies, titled "3D Printing", have revolutionized the design and fabrication processes in the manufacturing sector. As compared to conventional subtractive manufacturing methods, these novel technologies are all based on an additive manufacturing process in which parts are built layer-by-layer from the bottom up. This enables the fabrication of complex designs with high scalability and minimized material waste. Additive manufacturing processes have been used to print powder materials (Selective Laser Sintering), solid materials (Laminated Object Manufacturing), liquid materials through extrusion processes (Fused Deposition Modeling) and liquid materials through polymerization processes (Stereolithography) (Bartolo 2011).

Stereolithographic 3D Printing, developed by 3D Systems in 1986, is a solid freeform fabrication technology based on the polymerization of photopolymer resins via exposure to light. As with most additive manufacturing technologies, the first step in fabricating a 3D structure by stereolithography is to create a digital model of the part, using computer aided design software (CAD) or a 3D digital scanner. The model is then converted to a standard tessellation language file format (STL) that describes the surface geometry of the 3D model. Specialized software is

used to virtually slice the model into sequential layers. The resulting information is then sent to the stereolithography apparatus (SLA) for layer-by-layer fabrication (Melchels 2010).

Two main schemes of stereolithography apparatus have been implemented in the fabrication of 3D photopolymer structures: scanning laser systems and digital light projection based systems. In the first of these schemes, a computer-controlled laser beam is rasterized across the photopolymer resin and cures 2D cross-sections of a 3D structure in a sequential manner. In digital light projection based systems, spatial light modulators such as digital micro-mirror devices are used to project 2D pixel patterns, allowing entire cross-sectional layers to be polymerized at once (Figure 2.1). Both these schemes are compatible with microfabricating 3D biological systems, but they require photopolymer resins with advantageous properties.

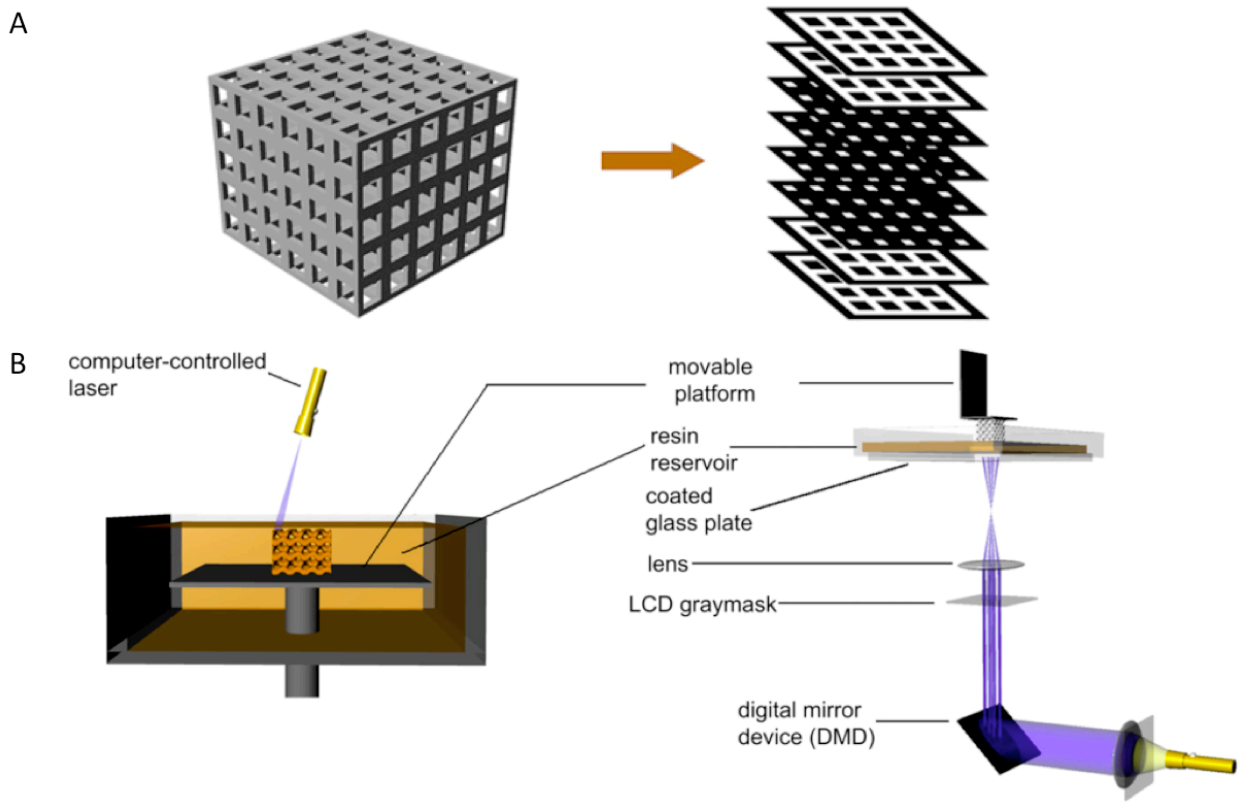

Figure 2.1: A) 3D Designs are sliced into sequential 2D cross-sections for layer-by-layer fabrication. **B)** Laser-based (left) and digital light projection based (right) systems are the most common stereolithography apparatus implemented in recent years (Melchels 2010).

2.1.3 HYDROGELS AS SYNTHETIC SCAFFOLDS FOR 3D CELL CULTURE SYSTEMS

There are a limited number of photopolymer resins for stereolithography that are compatible with applications in bionanotechnology. Among the most promising of these resins are the class of highly absorbent cross-linked polymeric structures known as "hydrogels". Hydrogels are a class of materials in which monomers undergo chemical and physical cross-linking to form polymer networks that are hydrophilic and biocompatible. The structural and functional properties of hydrogels, such as porosity and swelling behavior, can be readily tailored via modifications to the monomers on which their polymeric network is based. The porous and absorbent nature of these materials facilitates the diffusion of signals and nutrients through the polymeric network, leading to their wide use in biological and biomedical applications (Stampfl 2011). These solvent-swollen cross-linked polymer networks also have the ability to respond to changes in temperature, pH, illumination, or other physical and chemical stimuli. This is particularly advantageous for biomedical applications that rely on real-time response behavior such as dynamic medical implants or bioactuators that generate force in response to external stimuli (Hinkley 2004).

The suitability of hydrogels as synthetic scaffolds for engineering three-dimensional substitutes for native tissue and organs has been extensively explored in the literature (Peppas 2006). The mechanical properties of hydrogels resemble those of natural tissues, rendering them particularly attractive for applications in programmable tissue engineering. Cells that have been encapsulated in natural hydrogels, such as collagen and fibrin, as well as synthetic hydrogels such as poly (ethylene glycol) diacrylate, have been shown to survive and proliferate within these matrices in long-term studies. Natural hydrogels have the advantage of promoting cellular functions via a myriad of endogenous factors that are advantages for the viability and development of cells. Synthetic hydrogels have the advantage of having very well defined and tunable material properties that can be readily studied to determine the effect of individual signals on cellular function (Tibbit 2009).

Many synthetic hydrogels that have been tested as 3D cell culture platforms. Of these, poly (ethylene) glycol diacrylate (PEGDA) hydrogels are promising in their ability to maintain viability of encapsulated cells and sustain proliferation *in vitro* (Bryant and Anseth 2002, Williams 2003, Yeh 2006). Such hydrogels can be conjugated with bioactive moieties that enable different functional behaviors such as universal or cell-type selective adhesion and

targeted enzymatic degradation (Figure 2.2). These properties render PEGDA an attractive biomaterial for fundamental studies of cell mechanics and applications in tissue engineering, regenerative medicine, and drug delivery (Stephens-Altus 2011).

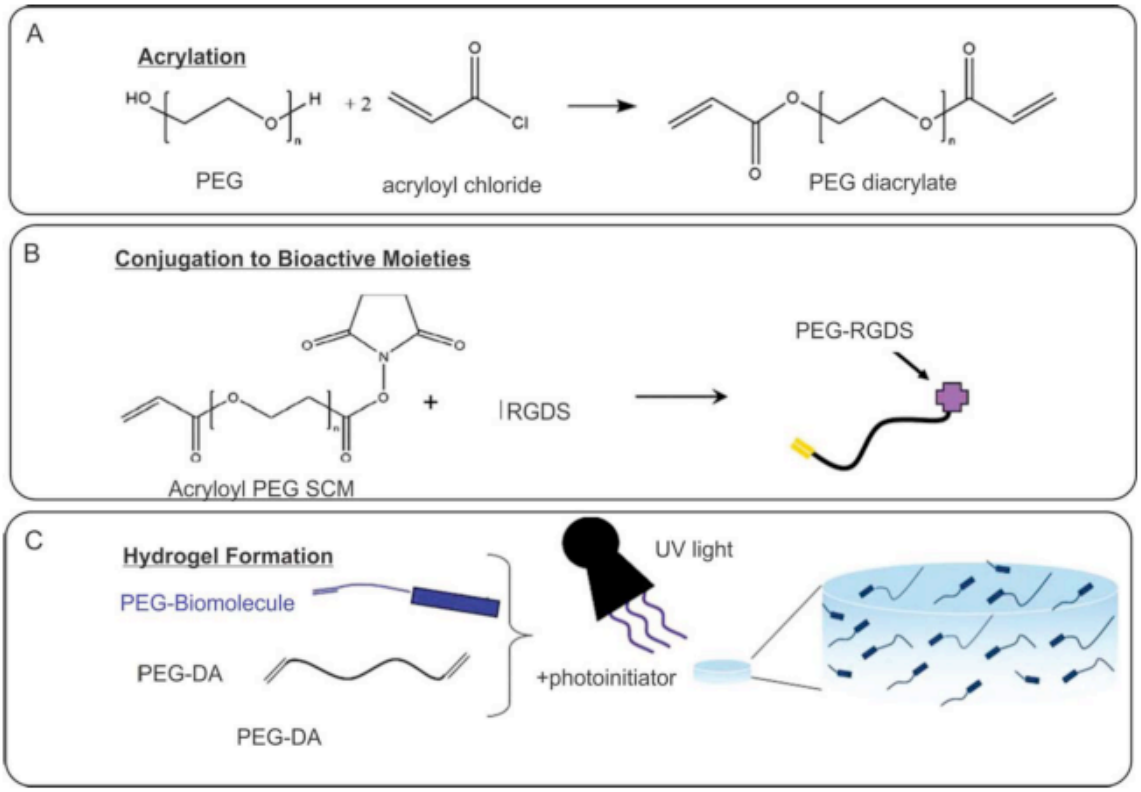

Figure 2.2: A) Addition of acrylate groups to PEG polymers generates the underlying structure for fabricating photocrosslinkable hydrogels. **B)** Incorporation of bioactive moieties, such as the Arg-Gly-Asp-Ser (RGDS) peptide series, can render hydrogels cell adhesive. **C)** Photocrosslinkable PEGDA hydrogels can be polymerized via exposure to ultraviolet light in the presence of a photoinitiator (Stephens-Altus 2011).

2.1.4 Stereolithographic Microfabrication of 3D Cell Culture Systems

Many researchers have investigated the microfabrication of poly (ethylene glycol) diacrylate (PEGDA) structures using 3D printing approaches (Ovsianikov 2010, Gaebel 2011). The studies that have proven most successful in their ability to encapsulate cells in 3D Printed PEGDA hydrogels have been based on stereolithography systems. Initial studies in this field utilized laser-based stereolithographic systems in which cells mixed with PEGDA prepolymer

solution were patterned via curing of the photopolymer in response to visible or ultraviolet light exposure (Figure 2.3) (Arcaute 2006, Chan 2010, Zorlutuna 2011). Photoinitiators that operate in the visible and ultraviolet regime have been well characterized for their effect on cure kinetics and cell toxicity in multiple studies (Williams 2005, Fairbanks, 2009, Bryant 2012). Of these, the visible light photoinitiator lithium phenyl-2,4,6-trimethylbenzoylphosphinate (LAP) and the ultraviolet light photoinitiator 2-hydroxy-1-[4-(2-hydroxyethoxy) phenyl]-2-methyl-1-propanone (I2959) are the most commonly used for encapsulation of living cells in 3D PEGDA polymeric networks (Fairbanks 2009).

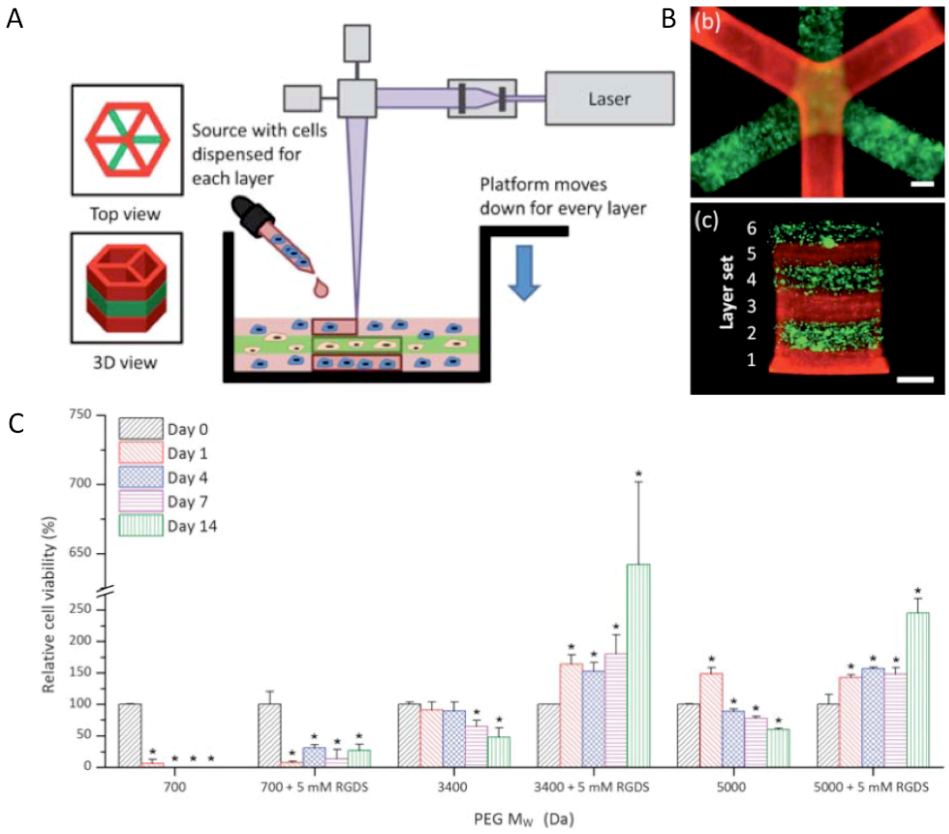

Figure 2.3: A) Schematic representation of cell encapsulation in PEGDA hydrogels via conventional laser-based stereolithography apparatus systems. **B)** 3D multi-material patterning of viable cells stained with either CellTracker® CMFDA (green) or CMTMR (orange) dye. Scale bars are 1mm. **C)** Viability of fibroblasts assessed over a period of 14 days for cells encapsulated in PEGDA hydrogels of varying molecular weights with or without incorporation of bioactive RGDS peptide sequence moieties (Chan 2010).

Recently, the development of projection micro-stereolithography systems (μSLA) have demonstrated the ability of this high-throughput, scalable technology to pattern photopolymers in complex 3D architectures (Sun 2005, Choi 2009, Xia 2009). These μSLA systems conventionally rely on a digital micro-mirror device (DMD) to serve as a dynamic mask for polymerization. This technology soon developed to include studies of patterning biocompatible polymers as scaffolds for 3D cell culture (Zhang 2012, Gauvin 2012, Grogan 2013, Lin 2013) as well as studies of cells encapsulated in hydrogel polymeric networks via μSLA (Soman 2013).

Most stereolithography systems used to encapsulate cells in hydrogels, both laser-based and digital light projector-based, rely on thorough mixing of the cells in the prepolymer solution to evenly distribute cells throughout the polymerized structure. These techniques offer some control over the architecture of cell-cell interactions within a polymerized hydrogel network, but a greater degree of precision over cell patterning enables more rigorous studies of cell mechanics and functionality *in vitro*. To this end, researchers have attempted to integrate higher precision cell patterning techniques in tandem with hydrogel photopolymer patterning. Examples of these techniques include biochemical surface modification of hydrogels via controlled protein patterning (Hynd 2007, Chan 2012), optical trapping of live cells followed by encapsulation in photopolymerizable hydrogels (Chiou 2005, Mirsaidov 2008, Linnenberger 2013), dielectrophoretic control of live cells followed by encapsulation in photopolymerizable hydrogels (Fan 2008, Bajaj 2012), and even magnetic cell levitation in 3D hydrogel tissue culture systems (Souza 2010).

Since the development of 3D printing technologies, the advantages of this novel additive manufacturing approach have been demonstrated for applications in a wide array of disciplines. The application of stereolithographic 3D printing to encapsulation of living cells in hydrophilic and biocompatible polymeric hydrogel networks have established this technology as an enabling tool in the field of biological and biomedical engineering. By giving researchers the ability to precisely control the spatiotemporal architecture of cell-cell and cell-matrix interactions as governed by physiology, the use stereolithography for fabricating 3D cell culture systems promises to revolutionize the fields of engineering and biology in the coming years.

2.2 TISSUE ENGINEERING: REVERSE ENGINEERING OF BIOLOGICAL SYSTEMS

2.2.1 INTRODUCTION TO CHALLENGES AND OPPORTUNITIES IN TISSUE ENGINEERING

One of the major applications of microfabrication of 3D cell culture systems is in the field of tissue engineering. Tissue engineering aims to create complex biological substitutes for native tissue using a combination of cells and instructive biomaterials. This emerging field promises to revolutionize modern medicine by providing an alternative to tissue and organ transplantation, and perhaps eliminating the need for transplants altogether by aiding the rapid development and testing of new drugs and therapies (Griffith 2002).

The conventional approach to tissue engineering has been the fabrication of porous degradable scaffold structures as platforms for cell seeding. In these studies, the scaffolds are often generated using conventional microfabrication approaches for patterning natural and synthetic materials (Zhang 2005). Researchers have even explored approaches in which cadaveric tissue is de-cellularized and repopulated with living cells to yield functional tissue and whole organs (Figure 2.4) (Ott 2008, Song 2013).

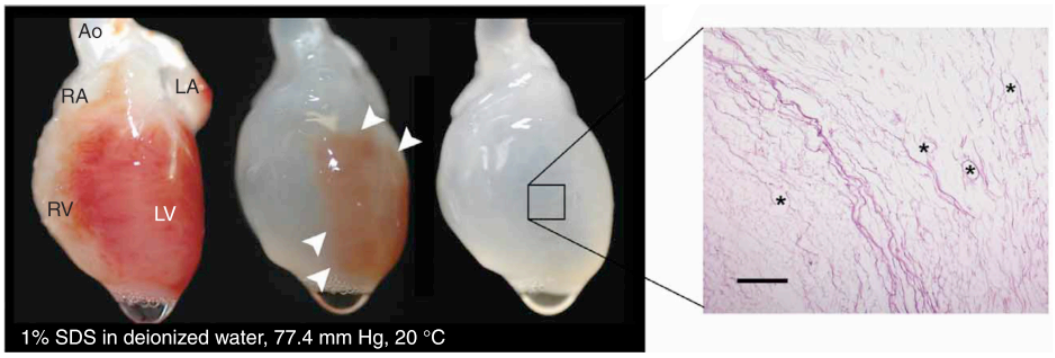

Figure 2.4: Cadaveric rat hearts perfused with SDS over a period of 12 hours yield de-cellularized scaffolds that maintain the large vasculature conduits present *in vivo* (represented by black asterisks in H&E stain). Repopulation of these scaffolds with living cells yielded macroscopic contraction of tissue engineered hearts (Ott 2008).

These scaffold-based approaches have the advantage of placing cells within a precise morphological design while maintaining the cell-cell and cell-matrix interactions that are seen *in vivo*. However, these approaches come with the challenges of regulating the distribution of cells

within the scaffolds, as well as the inability to engineer adequate vascular networks that can provide supplies of nutrients to large-scale engineered tissues. These challenges render scaffold based "top down" approaches undesirable for applications in tissue engineering of complex tissues and organs, as they are unable to provide precise spatial control of cells and biochemical signals in three dimensions (Andersson 2004).

The rise of "bottom up" approaches in microfabrication, triggered by the advent of additive manufacturing technologies, provides an attractive alternative approach to manufacturing complex biological substitutes for native tissue and organs. Assembling tissues layer by layer from the bottom up using 3D printing technology will allow for complex three-dimensional control over the morphological and functional properties of engineered tissue. Additionally the scalability, high reproducibility, cost effectiveness, and ease of customization of 3D printing technologies render this an attractive approach to providing individually tailored biological substitutes for native tissue.

2.2.2 3D PRINTED 3D CELL CULTURE SYSTEMS FOR TISSUE ENGINEERING

Many microfabrication approaches for tissue engineering applications have been explored in recent years. These approaches come with the advantage of high-throughput and reproducible experimentation that offers precise spatiotemporal control of cell signaling and culture conditions *in vitro*. Applications of such technologies in the field of pancreatic, liver, cartilage, vasculature, nerve tissue, cardiac and skeletal muscle engineering have demonstrated rapid progress towards the goal of reverse engineering native tissue and organs (Khademhosseini 2006, Park 2007, Vunjak-Novakovic 2010).

Pioneering studies in bottoms-up tissue engineering have used 3D bio-printing to deposit "bio-ink" spheroids containing live cells into a supportive hydrogel environment and allowing the printed cells to self-assemble into topologically defined three-dimensional structures (Figure 2.5) (Mironov 2007, Jakab 2008, Norotte 2009). These techniques allow cells to be arranged at high densities in physiological relevant morphologies and culture conditions. Similar systems that build tissue layer by layer from the bottom up via inkjet or nozzle based printing systems have proved promising for engineering cartilage and bone *in vitro* (Cohen 2006, Boland 2006). While many of these technologies are able to engineer tissue constructs with spatially

homogenous material and functional properties, they are still far from achieving the degree of complex 3D control required to replicate native tissue architecture (Sawkins 2013).

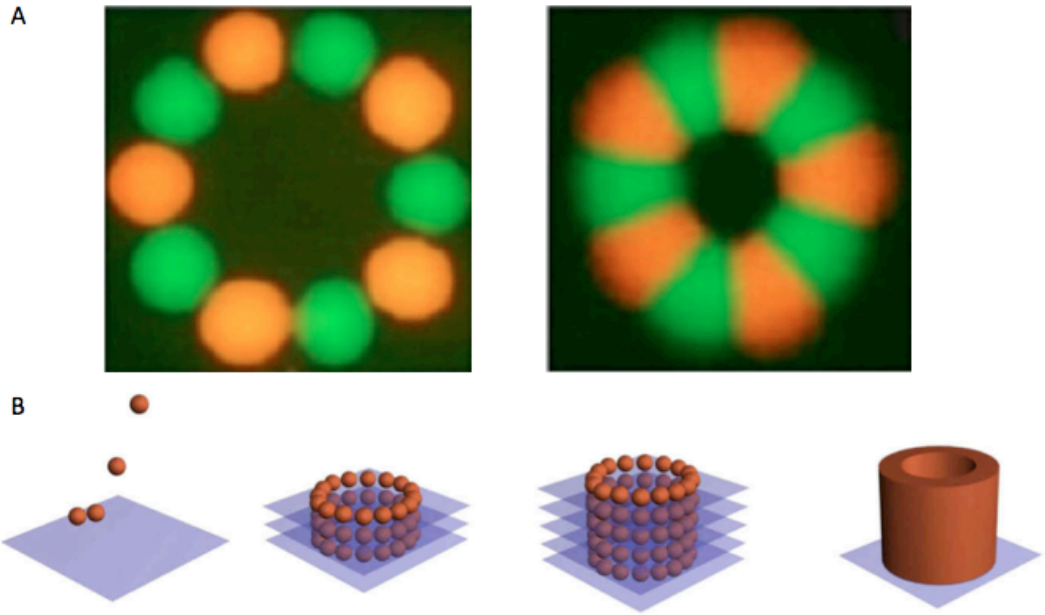

Figure 2.5: A) "Bio-ink" spheroids printed into a circle fuse into a 3D toroid after ~60 hours; **B)** Schematic of 3D tissue constructed via sequential layer-by-layer spheroid deposition and fusion.

The stereolithographic 3D printing systems presented earlier in this chapter are ideal candidates for targeting applications in bottom-up tissue engineering. SLA systems have demonstrated capabilities in high resolution patterning of photopolymers and have the advantageous property of being able to encapsulate cells in polymeric networks while preserving viability and functionality in long-term studies. Additive photopatterning of PEGDA hydrogels has been shown to be a viable method of engineering 3D substitutes for native tissue (Tsang 2007, Du 2008). The use of SLA based systems for directing the growth of microvasculature have also been explored, promising to provide perfusable networks for nutrient supply in large-scale structures (Jeong 2012). However, much remains to be explored in the field of stereolithographic 3D printing systems that specifically target engineering substitutes for native tissue and organs. This enabling microfabrication technology thus promises to drive the next era of programmable tissue engineering for applications in medicine and biology.

2.3 BIOLOGICAL MACHINES: FORWARD ENGINEERING OF BIOLOGICAL SYSTEMS

2.3.1 INTRODUCTION TO FORWARD-ENGINEERED LIVING MACHINES

The field of reverse engineering biological systems for applications in tissue engineering and regenerative medicine has garnered much success in recent years. However, progress in this field is hampered by the lack of fundamental understanding on how cell-cell and cell-matrix interactions in complex 3D networks lead to larger, system-level functional response. It is anticipated that studies that focus on building novel biological systems from the "bottom up" will allow researchers to capture the complex interactions between systems at the micro- and macro-scale. Reverse engineering as a method for recapitulating the structure of existing biological tissues and organs goes some way towards addressing the challenges in this field. However, it has also driven the formation of a new field in tandem: "forward engineering" of biological machines and systems.

Forward engineering is focused on designing novel systems that harness the innate dynamic abilities of biological systems to self-organize and respond to environmental cues. The ultimate goal of these efforts is to engineer integrated cellular systems, or "living machines", that combine knowledge from the diverse disciplines of engineering design and manufacturing, bionanotechnology, tissue engineering, and synthetic biology to sense, process, and respond to signals in a dynamic environment. Such multi-functional machines, built from the modular components of biological tissue, can address many challenges and applications (Kamm 2013). Applications in cell-based soft robotics, in which living machines are designed to accomplish such objectives of robotics as sensing, storage and processing of signals, and a resultant response such as actuation, have generated much interest in recent years.

Perhaps the most intuitive demonstration of a "living machine" is a biological system that can generate force and produce motion. To that end, many studies have explored the use of existing biological components as power sources that drive the actuation of machines of multiple length scales ranging from the nano- to macro-scale regimes. Pioneering studies in this field investigated nano-scale actuation of the motor proteins kinesin and myosin, which use adenosine triphosphate (ATP) as a source of fuel for generating force and demonstrating motility (Vale 1985, Spudich 1994). Applications of such molecular motors as nano-scale machines have been explored, in which the tension-sensing capabilities of myosin motors demonstrate its

advantageous properties as a molecular force sensor (Laakso 2008). Further studies in this field delved deeper into applications of existing biological systems as actuators by employing strands of DNA molecules to drive the actuation of nano-machines. In these machines, strands of DNA assembled to form shapes resembling tweezers were placed in solution with auxiliary strands of "fuel" DNA. The subsequent hybridization of DNA strands generated force and drove opening and closing of the tweezer-like living machines (Figure 2.6A) (Yurke 2000, Simmel 2001).

On the micro-scale, single cells or swarms of cells have been used to drive the actuation of robotic devices in fluidic systems. Bacterial cells have been shown to generate force and drive actuation and locomotion of micro-scale robotic devices (Martel 2006). Control of these bacterial cells via magnetotactic and chemotactic mechanisms have opened up applications in which living machines can sense and process external signals in order to generate a resultant response (Kim 2012). Similarly, researchers have explored the use of motile sperm cells as actuators for locomotion of micro-robots. In these studies, the force production of sperm flagella has been used as a biological power source for motility in a fluidic environment (Magdanz 2013).

Use of existing biological components on larger scales, corresponding to the size of living tissue and organs, have also been explored as actuators for macro-scale devices. Recent studies that investigate the use of heart muscle tissue excised from live insects as a source of fuel have demonstrated that the spontaneous contraction of this tissue can drive actuation of tweezer-like manipulators (Figure 2.6B) (Akiyama 2013).

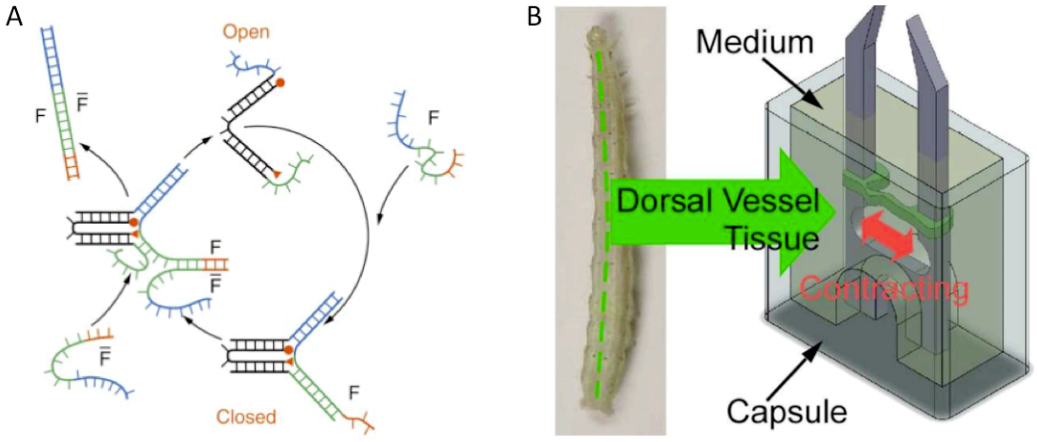

Figure 2.6: A) Tweezer-like living machine powered by the hybridization of DNA strands (Yurke 2000); **B)** Tweezer-like bio-hybrid machine powered by the contraction of heart muscle tissue excised from a live insect (Akiyama 2013).

Living machines that are powered by existing biological systems, as explored in the previous sections, are advantageous in that they demonstrate the ability to fabricate soft robotic devices that are driven by a variety of easily controllable signals and have the dynamic response and self-healing properties found in biological systems. However, because they rely on the direct use of existing systems, they limit the design parameters of micro-robotic devices. True forward engineering of living biological machines requires a greater degree of control over the design and functionality of bioactuators. These machines could even potentially surpass the force generation and actuation behaviors found in native tissue, leading to a new era of design in which biological materials will be an accepted component of every engineer's "toolbox".

2.3.2 CARDIAC MUSCLE AS A BIOACTUATOR

Cardiac muscle *in vivo* is designed to act as a pump that drives blood flow through vasculature. The high density of cells in native myocardium allows for the formation of a syncytium, enabling the coordinated propagation of electrical signals that leads to synchronous contraction of the tissue (Vunjak-Novakovic 2010). This advantageous property renders cardiac muscle an attractive tissue for applications in bioactuation.

Tissue engineered cardiac muscle tissue for applications in regenerative medicine have been studied extensively in recent years, as the need to restore contractile function to hearts upon myocardial infarction, or "heart attack", is of great importance to the medical community. Studies have shown that engineered cardiac tissue grafts implanted onto infarcted rat hearts can electrically couple with native tissue and improve the systolic and diastolic function of diseased myocardium *in vivo* (Figure 2.7) (Zimmerman 2006). This and other studies have provided evidence that engineered cardiac tissue can mimic the contractile function of native tissue, leading to ongoing human clinical trials focused on using engineered muscle tissue to treat cardiomyopathy.

Since the contractile behavior of muscle tissue is driven by the propagation of electrical signals known as action potentials, engineered cardiac muscle tissue can be stimulated and paced *in vitro* via electrical signals that mimic those in native heart tissue. Electrical signaling during development of engineered tissue has even been shown to enhance the cell differentiation and functional assembly of the tissue, leading to the formation of conductive and contractile properties that mimic native myocardium (Radisic 2004). Such tissues have been explored as

useful tools for applications in disease modeling and high-throughput drug screening *in vitro*. In these studies, engineered cardiac tissues that have been exposed to drugs with known cardiotoxic effects and stimulated via electrical signaling demonstrate dose-dependent contractile responses to the administered drugs. The ability to control the contraction and pacing of engineered cardiac tissue with electrical stimulation thus has many practical applications (Iyer 2011).

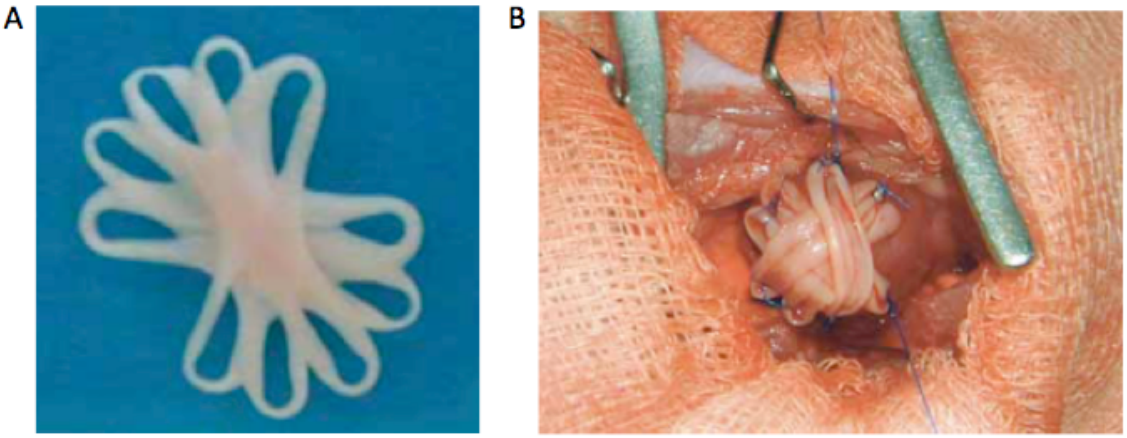

Figure 2.7: A) Multiple loops of engineered heart tissue combine to form a contractile tissue graft; **B)** Tissue grafts implanted onto infarcted rat hearts support contractile function.

Conventional approaches to engineering cardiac tissue have focused on either the cell sheet engineering approach or the cell scaffold approach. The cell sheet engineering approach generally involves plating a sheet of cardiac tissue on a 2D substrate, promoting the formation of planar cell-cell junctions that help the tissue beat in synchrony upon electrical stimulation. Such tissues have recently been used as actuators for locomotion of biorobotic devices.

A pioneering study in this field engineered a sheet of cardiac tissue on a synthetic elastomer designed to form a quasi-closed "bell" structure. Electrically controlled contraction of the engineered cardiac tissue alternately contracted and relaxed the elastomer body, leading to propulsive swimming behavior that mimicked the movement of jellyfish (Figure 2.8A). Qualitative and quantitative comparisons of this biomimetic movement to that of real jellyfish demonstrated that the engineered system was able to replicate the momentum transport and body lengths traveled per swimming stroke of the natural system (Nawroth 2012).

Another study in this field engineered sheets of cardiac tissue on hydrogel cantilevers fabricated using a 3D printer (Figure 2.8B). The autonomous and synchronous contraction of the

cardiomyocytes led to a change in conformation of the cantilever structures, leading to an inch worm-like biomimetic walking motion (Chan 2012).

Similar studies of engineered cardiac tissues seeded on hydrogel substrates have investigated the effects of incorporating nano-scale fibers and carbon nanotubes into the hydrogel substrates. These embedded materials improve the mechanical integrity of the substrate material and, by providing the engineered tissue with an electrically conductive nanofibrous architecture that mimicked the *in vivo* environment, been shown to enhance the functional performance of cardiac cell sheets (Kharaziha 2013, Shin 2013).

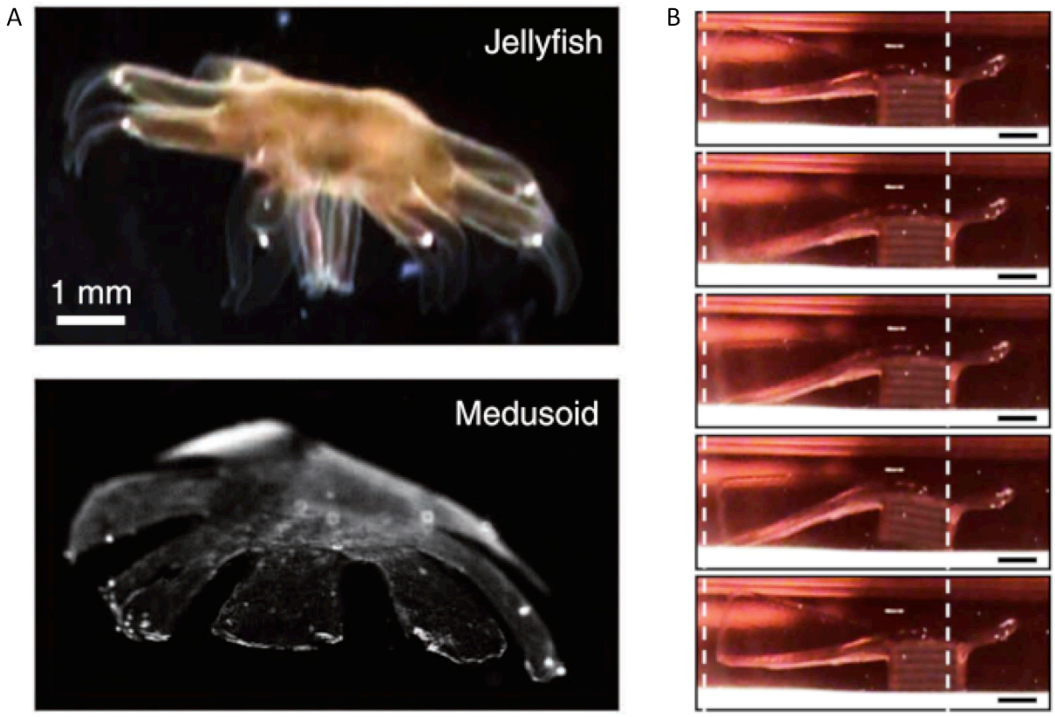

Figure 2.8: A) Engineered sheet of cardiac muscle seeded on a soft substrate, termed a "medusoid" fuels a propulsive swimming mechanism in this living machine that mimics the motion of a jellyfish (Nawroth 2012). **B)** Engineered sheet of cardiac muscle seeded on a 3D printed hydrogel structure drives an inch-worm like biomimetic crawling motion across a substrate (Chan 2012).

An alternative to engineering sheets of cardiac tissue has been engineering cells in a scaffold to form a 3D strip of muscle. A pioneering study in this field seeded cardiomyoctes in a collagen gel cast to form ring-like 3D structures capable of contractile function. These

engineered tissues displayed electrophysiological properties similar to those found in native cardiac tissue (Eschenhagen 1997). More recent studies of engineered cardiac microtissues seeded in fibrin and collagen gels have investigated the functional behavior of these tissues. In these studies, engineered cardiac tissue is tethered to cantilevers that deflect in response to muscle contraction (Boudou 2011). In addition to acting as a force sensor, such cantilever-based mechanisms demonstrate the use of engineered cardiac tissue as a bioactuator capable of force generation and contractility.

Thus, while engineering of cardiac tissue has historically been driven by applications in regenerative medicine, the studies generated in this field have demonstrated the power of cardiac muscle to act as an actuator for other applications. It is anticipated that the future of forward-engineered bio-robotic devices will utilize engineered cardiac tissue as a source of fuel and force production.

2.3.3 SKELETAL MUSCLE AS A BIOACTUATOR

While cardiac muscle tissue has many advantageous properties that make it an appealing choice for bioactuator applications, much research has been done in tandem on the use of skeletal muscle tissue for applications in this field. Skeletal muscle *in vivo* has a highly organized and hierarchical tissue architecture. Individual muscle cells, termed myoblasts, differentiate into multicellular elongated structures, myotubes, which are capable of contractility. These myotubes form muscle fibers that are aligned in bundles termed fascicles. The muscle fascicles in turn combine to form the macro-scale structure of skeletal muscle. This high degree of organization and alignment on the micro- and macro-scale allows skeletal muscle to efficiently generate force and produce motion. Indeed, skeletal muscle can generate over 200 kPa of stress and sustain 20% strain, properties that no currently available actuator of a similar size can mimic (Neal 2013). Unlike cardiac tissue, skeletal muscle does not show significant spontaneous contractile behavior, making it easier to control the contractility of engineered skeletal muscle tissue via external signaling. Furthermore, skeletal muscle cells can interface with multiple cell types, such as neurons and endothelial cells, making them an ideal platform for forward-engineering integrated cellular systems.

A pioneering study in the engineering of skeletal muscle tissue formed a sheet of primary muscle cells isolated from a rat and allowed the sheet to roll into a 3D strip of muscle capable of

contractility and force generation in response to electrical signaling (Dennis 2000). This study was followed by experiments that investigated contractile behavior of muscle cells seeded in synthetic extracellular matrices such as fibrin gels, which have a stiffness similar to that of native muscle tissue (Huang 2005, Khodabukus 2009). Electrical stimulation of these engineered muscle tissues demonstrated that engineered muscle is capable normal physiological function in length-tension and force-frequency relationships. However, engineered muscle produces significantly less force per unit cross-sectional area as compared to native skeletal muscle.

Investigations of the biological architecture of engineered skeletal muscle tissue have shown that engineered tissue mimics native tissue by forming striated sarcomere structures, the smallest contractile units found in skeletal muscle (Fujita 2007). Moreover, muscle cells cultured in fibrin gels subjected to strain formed highly aligned myotubes and bundle-like structures in the direction of the applied strain, similar to morphology seen *in vivo* (Matsumoto 2007).

Building on this early work, studies of muscle cells in fibrin gel matrices investigated the use of microfabricated molds to guide the alignment and differentiation of densely packed myofibers (Bian 2009). Increased alignment of muscle fibers in engineered tissue led to a significant corresponding increase in the force produced by the tissue constructs (Lam 2009). Furthermore, directed patterning of mechanical stress in these engineered tissue structures led to the formation of controllable gradients of extra cellular matrix protein compositions and organization with 3D engineered tissue (Legant 2009).

The matrix compositions of both fibrin and collagen gels that lead to force generation capacity comparable to native tissue has been extensively characterized and optimized (Hinds 2011). These and other studies have contributed to significant advances in this field, providing researchers with the ability to engineer skeletal muscle tissue that reproducibly mimics the complex morphological organization and functional behavior of native tissue (Figure 2.9). The ability of these engineered tissues to efficiently generate force and produce motion makes them ideal bioactuators for applications in forward-engineered robotics.

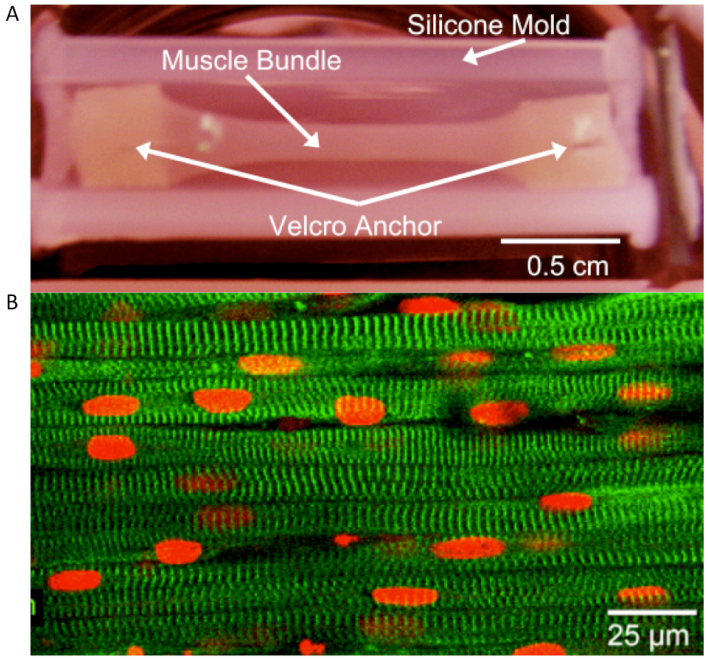

Figure 2.9: A) Bioengineered skeletal muscle bundle formed within synthetic hydrogel capable of force generation and contractility; **B)** Highly organized structure of engineered muscle shows aligned multi-nucleated myotubes (red nuclei) exhibiting cross-striations characteristic of sarcomeric structures *in vivo* (red) (Hinds 2011).

2.3.4 Controlled Behavior of Forward Engineered Bioactuators

In order for engineered muscle tissues to be used as actuators for force production and locomotion of robotic devices *in vitro*, they must be readily controllable via external signaling. The studies outlined in the previous sections primarily utilize electrical signals to drive contractility of both cardiac and skeletal muscle tissues. While this is certainly an effective signaling method, electrical signaling is disadvantageous in that it cannot be used to precisely target precise regions of tissues.

Optogenetic technology has recently garnered much interest as a method of achieving targeted control over cellular behavior. This technology is based on incorporating genes that code for light-sensitive ion channels, such as Channelrhodopsin-2, into cellular membranes. This renders it possible to control membrane voltage potential via optical signaling, thereby providing a noninvasive method of externally triggering the generation of action potentials in muscle tissue (Deisseroth 2011). By contrast with electrical signaling, optogenetic signaling allows for highly precise spatiotemporal control of stimulation.

Light-sensitive ion channels incorporated into cardiac and skeletal muscle tissues are just beginning to be explored for application in bioactuation. A recent study of skeletal muscle tissue formed in fibrin gels, as in the studies previously considered, utilized myoblasts from the C2C12 cell line that had been transfected with Channelrhodopsin-2, an ion-channel that is sensitive to blue light of 490 nm wavelength. The 3D tissues formed in this study were anchored by microfabricated cantilever posts and stimulated to contract via pulsed blue light. The resulting deflection of the posts in response to the active tension generated by the muscle was measured and converted into a value of force (Figure 2.10) (Sakar 2012). Following these preliminary studies, other experiments have demonstrated precision of the optogenetic targeting method and its ability to convert light energy into mechanical actuation via wireless and non-invasive external signaling (Neal 2013).

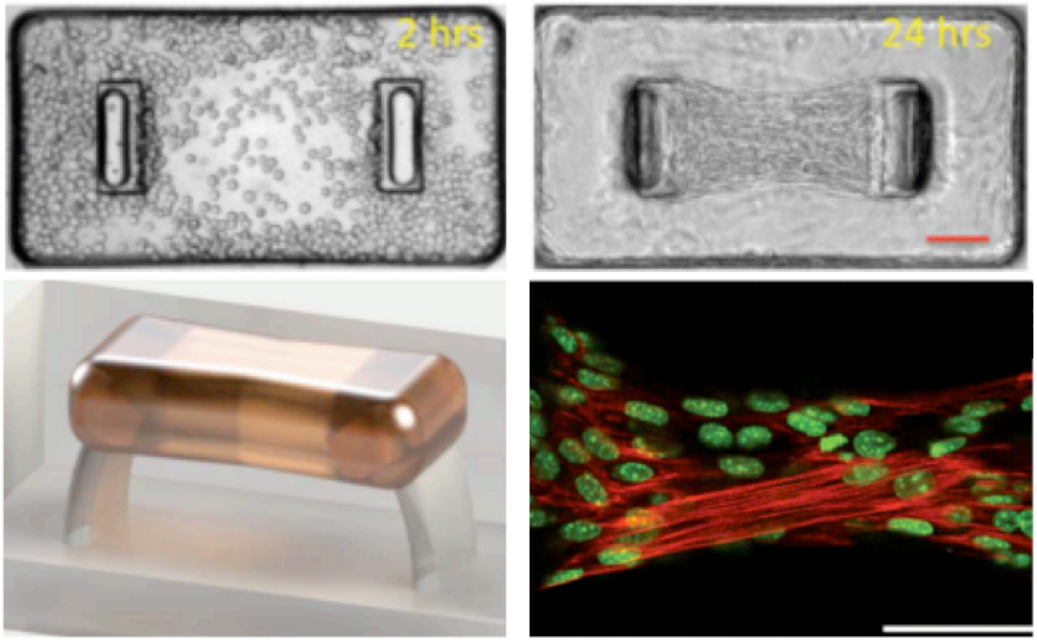

Figure 2.10: C2C12 muscle cells transfected with light-sensitive ion channels and seeded in a fibrin gel remodel into a 3D strip of engineered muscle over time that mimics the morphological and functional behavior of native muscle tissue. Deflection of the cantilever posts to which the muscle is anchored yields a quantitative characterization of force generation in response to optical and electrical stimulation (Sakar 2012).

Forward-engineered biological systems require the integration of multiple cell types in order to perform complex sensing and actuation tasks. For example, *in vivo*, muscles are

controlled via complex neural circuits that interface with muscle via neuromuscular junctions. Efforts to engineer a functional neuromuscular junction *in vitro* have very recently met with success. In a recent study, researchers differentiated mouse neural stem cells into functional motor neurons that formed synaptic connections with engineered skeletal muscle. Glutamic acid activation of the neurons triggered active potentials and subsequent contractions in the muscle (Morimoto et al).

In similar efforts to integrate multiple cell types into engineered systems, many research groups have explored integrating perfusable vascular networks into engineered tissue to mimic the complex transport mechanisms seen *in vivo.* Pioneering studies in this field have demonstrated long-lasting perfusable blood vessels that remain stable and functional when implanted *in vivo* (Koike 2004). Studies of microfabricated perfusable vascular networks via techniques that are compatible with a variety of cell types and synthetic and natural extracellular matrices have also met with success (Miller 2012). However, demonstrations of truly integrated biological systems composed of multiple cell types are in a very nascent stage of development.

It is likely that future studies in this field will rely on differentiation of pluripotent stem cells into multiple lineages to form truly integrated cellular systems capable of complex functional behaviors. Studies of differentiating stem cells into multiple lineages have recently garnered much momentum, leading to the development of "organoids" with morphological organization that mimics native tissue (Bershetyn 2013). Application of these technologies to create cardiac muscle based bioactuators have been demonstrated (Thavandiran 2013), and future research on biological machines and systems will likely use these approaches as enabling tools in the fabrication of integrated multi-cellular systems.

The goal of engineering functional tissues that can sense, process, and respond to signals while maintaining metabolic function over long periods of time comes with many diverse challenges. While great advances have been made in engineered functional bioactuators that can be precisely controlled and interfaced with multiple cell types, there are many technological hurdles that must be overcome in order to create systems that can self-organize, self-heal, and even self-replicate in response to complex external cues. Stereolithographic microfabrication has been proposed as a method for engineering 3D cell culture systems *in vitro*. The use of this technology as an enabling tool in engineering biological machines and systems shall be illustrated in this thesis.

CHAPTER 3: 3D MICRO-STEREOLITHOGRAPHIC PRINTING

3.1 INTRODUCTION

Cells *in vivo* are arranged in precise three-dimensional architectures and surrounded by a range of biochemical and mechanical signals that promote cell-cell and cell-matrix interactions and control functional behavior. In order to gain a quantitative understanding of the way cells sense, process, and respond to signals in their environment, we need to develop *in vitro* model systems that can accurately replicate the structure and function of native tissue. These model systems could have a range of applications including high throughput drug testing, tissue engineering and regenerative medicine, fundamental studies of disease development, and the fabrication of biological machines and systems.

Engineering *in vitro* model systems that recreate the structure and function of native tissue requires the ability to pattern cells and cell signals at physiologically relevant length scales. This motivates the development of a 3D printing apparatus capable of patterning cells and cell signals at high resolution, on the order of single cells (1-50 μm). While there have been many demonstrations of using a stereolithography apparatus to pattern cells encapsulated in highly absorbent hydrogel photopolymers, few have been able to fabricate complex three-dimensional structures at resolutions on the order of cells in the body (Soman 2013).

In this study, a custom-built projection micro-stereolithography apparatus was used to pattern hydrogel polymers at resolution < 10 μm. Hydrogels were patterned into 3D structures in which distinct layers demonstrated the multi-material patterning abilities of this apparatus. Long-term viability of NIH/3T3 fibroblast and C2C12 murine myoblast cells encapsulated in these patterned hydrogels was evaluated over a period of 7 days.

3.2 MATERIALS AND METHODS

3.2.1 PROJECTION MICRO-STEREOLITHOGRAPHY APPARATUS

A projection micro-stereolithography apparatus (μSLA) for high-resolution patterning was designed and custom-built for this study (Figure 3.1). In this apparatus, broad-spectrum light from a lamp (X-Cite 120Q, Lumen Dynamics, Mississauga, Ontario, Canada) is channeled

through a liquid-filled light guide and filtered through a collimating adaptor (Zeiss Axio Standard, BioVision Technologies, Exton, PA, USA). The resulting collimated light is filtered through a UV-passing colored glass filter (UG11, Thor Labs, Newton, NJ, USA) and focused through a UV-coated lens (LA1256-A, Thor Labs, Newton, NJ, USA). The light is then filtered through two polarizers onto a spatial light modulator (SLM) isolated from a DLP-based projector (PowerLite S5, Epson, Suwa, Japan). The filtered light is collected and focused through another UV-coated lens (LA1301-A, Thor Labs, Newton, NJ, USA) onto a UV-enhanced aluminum turning mirror (CM1-F01, Thor Labs, Newton, NJ, USA) placed within a microscope (Epiphot 200, Nikon, Tokyo, Japan). Finally, the light is further focused through a 10X microscope objective onto the polymerization stage of the μSLA.

A custom-made micrometer stage capable of 10 μm x-y-z resolution was built by combining standard stage apparatus (Mitutoyo, Kawasaki, Japan) and placed above the stage of the μSLA polymerization stage. This micrometer stage allowed for rasterizing the projected light pattern, giving the ability to create large millimeter scale structures with feature sizes on the order of single microns. Patterns for the SLM, which served as the dynamic "mask" for polymerization, were generated using gray-scale PowerPoint images (Microsoft, Redmond, WA, USA).

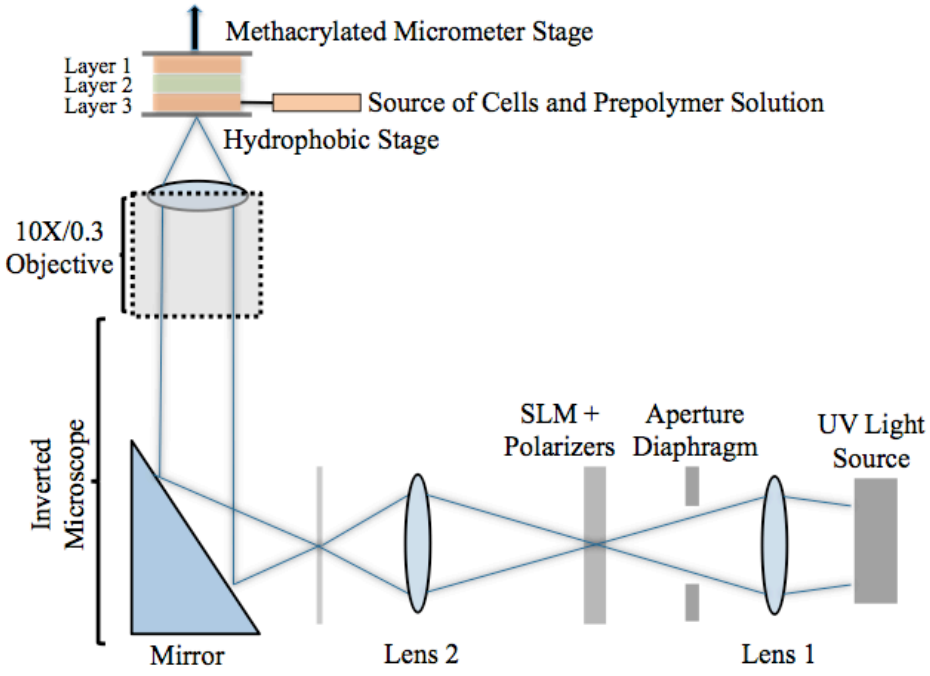

Figure 3.1: Schematic of projection micro-stereolithography apparatus

3.2.2 PRE-POLYMER PREPARATION

Poly(ethylene glycol) diacrylate (PEGDA) hydrogels of molecular weight 700 g mol^{-1} and 1000 g mol^{-1} (Sigma-Aldrich, St Louis, MO, USA) were patterned using the μSLA in this study. For studies of resolution without encapsulated cells, 20% (v/v) solutions of PEGDA 700 and 20% (w/v) solutions of PEGDA 1000 were prepared by dissolving the polymer in phosphate buffered saline (Lonza, Basel, Switzerland). A 50% (w/v) stock solution of photoinitiator was prepared by dissolving 1-[4-(2-hydroxyethoxy)-phenyl]-2-hydroxy-2-methyl-1-propane-1-one (Irgacure 2959, Ciba, Tarrytown, NY, USA) in dimethyl sulfoxide (DMSO, Fisher Scientific, Springfield, NJ, USA). This solution was added to the pre-polymer solution to form 0.5% (w/v) of photoinitiator for PEGDA 700 and 1.0% (w/v) for PEGDA 1000. Rhodamine-B fluorescent dye (R6626**,** Sigma Aldrich, St Louis, MO, USA) was added to the pre-polymer solutions for better visualization of small feature sizes. Cured hydrogels were allowed to swell for at least 1 hour in phosphate buffered saline (Lonza, Basel, Switzerland) prior to imaging and resolution characterization.

For studies of resolution with encapsulated cells, a 20% (w/v) solution of PEGDA 1000 was prepared by dissolving the polymer in Dulbecco's Modification of Eagle Medium (DMEM) with or without cells and with L-glutamine and sodium pyruvate without phenol red (Cellgro Mediatech, Herndon, VA, USA). The media contained 10% fetal bovine serum (FBS, Sigma Aldrich, St Louis, MO, USA), 1% penicillin-streptomycin and 1% L-glutamine (Cellgro Mediatech, Herndon, VA, USA). The photoinitator stock solution was added to the pre-polymer solution to form 1.0% (w/v) of photoinitiator.

3.2.3 ENERGY DOSE CHARACTERIZATION

Fluorescent microbeads of 0.4-0.6 μm diameter (Nile Red Beads, Spherotech, Lake Forest, IL, USA) were combined with hydrogel pre-polymer solution at a 1:200 volumetric ratio. Ultraviolet (UV) light was projected through a blank SLM screen to cure the hydrogel onto a glass slide attached to the polymerization stage. The UV light energy was measured using a digital power meter calibrated for 325-365 nm (FieldMate, Coherent, Santa Clara, CA, USA). The thickness of the cured hydrogel at different values of UV energy dose was measured using an inverted fluorescence microscope (IX81, Olympus, Center Valley, PA, USA) and IPLab software (BD Biosciences, Rockville, MD, USA). The measured thickness as a function of UV

energy dose was plotted on a semi-logarithmic graph and a linear regression analysis was used to characterize the relationship between energy dose and thickness.

3.2.4 3D PATTERNING

The polymerization stage of the μSLA apparatus was rendered hydrophobic by the application of Rain-X (Royal Dutch Shell, The Hague, Netherlands). Methacrylated surfaces were prepared via treatment of cover glass slides with 0.2% (v/v) 3-(trimethoxysilyl)propyl methacrylate (3-TPM, Sigma-Aldrich, St Louis, MO, USA) followed by a wash in 100% ethanol (Decon Labs, King of Prussia, PA, USA) and hard-baked on a hot plate at 110ºC. The methacrylated cover glass slides were attached to the micrometer stage. The hydrogel prepolymer solution was pipetted into the space between the polymerization stage and the methacrylated micrometer stage. Once the hydrogel was patterned and cured by the projected ultraviolet light, the micrometer stage was moved up in preparation for polymerization of the next layer. The polymerized hydrogel was chemically bonded to the methacrylated glass slide attached to the micrometer stage and hence did not adhere to the hydrophobic polymerization stage during processing. This method was used for layer-by-layer multi-material fabrication of 3D hydrogel structures.

3.2.5 CELL ENCAPSULATION AND VIABILITY ASSESSMENT

NIH/3T3 fibroblasts and C2C12 murine myoblasts were maintained in growth medium: DMEM with 10% fetal bovine serum (FBS, Sigma Aldrich, St Louis, MO, USA), 1% penicillin-streptomycin and 1% L-glutamine (Cellgro Mediatech, Herndon, VA, USA) in an incubator at 37ºC and 5% CO_2. Cells were trypsinized (TrypLE Express, Gibco, Carlsbad, CA) and resuspended at a concentration of 5E6 cells mL^{-1} in PEGDA 1000 pre-polymer solution formulated as described in a previous section. Immediately after preparation of the pre-polymer solution, the cells were patterned using the μSLA apparatus and placed in warm growth medium and incubated at 37ºC and 5% CO_2.

Viability was assessed via MTS colorimetric assay, in which a reaction between MTS (3-(4,5-dimethylthiazol-2-yl)-5-(3- carboxymethoxyphenyl)-2-(4-sulfophenyl)-2H-tetrazolium, Promega, Madison, WI, USA) and phenazine methosulfate (PMS, Sigma Aldrich, St Louis, MO, USA) produces a water-soluble purple formazan product as an indication of the presence of

living cells. An assay solution of MTS at a concentration of 333 μg mL^{-1} and 25 μM PMS dissolved in DMEM without phenol red was added to wells containing hydrogels with encapsulated cells patterned by the μSLA apparatus. The hydrogels were incubated in this assay solution for a period of 4 hours at 37ºC and 5% CO_2. After the incubation period, the assay solution was removed from the wells and pipetted into a separate well plate. Absorbance of the assay solution was measured at 490 nm using a microplate reader (BioTek, Winooski, VT, USA).

3.3 RESULTS

3.3.1 RESOLUTION CHARACTERIZATION OF PATTERNED HYDROGELS

The ultimate goal of building a projection micro-stereolithography apparatus is to microfabricate large millimeter-scale hydrogel structures with feature sizes on the order of single microns. In order to attain this high resolution, the energy dose of ultraviolet light required to cure the hydrogel pre-polymer solution must be precisely determined. Under-curing structures will result in low-fidelity polymers without resolved features that will disintegrate quickly. Over-curing structures will result in high-density cross-linking and swelling of the hydrogels that will overwrite existing small features.

To determine the optimal energy dose of ultraviolet light required to cure hydrogels with small feature sizes, it is necessary to characterize the relationship between ultraviolet energy dose and the thickness, or "cure depth", of the polymerized hydrogels. In this study, fluorescent micro-beads were encapsulated in the hydrogels and a fluorescence microscope was used to measure the thickness of polymerized parts, as described in Section 3.2.3. Thickness of poly (ethylene glycol) (PEGDA) polymers of molecular weight 700 g mol^{-1} and 1000 g mol^{-1} was plotted as a function of ultraviolet energy dose on a semi-logarithmic graph (Figure 3.2). A linear regression analysis was used to develop a characteristic equation for the μSLA apparatus. The R^2 values of 98.3% for PEGDA 700 and 97.3% for PEGDA 1000 indicate a strong correlation between the characteristic equation and the data generated by the μSLA apparatus.

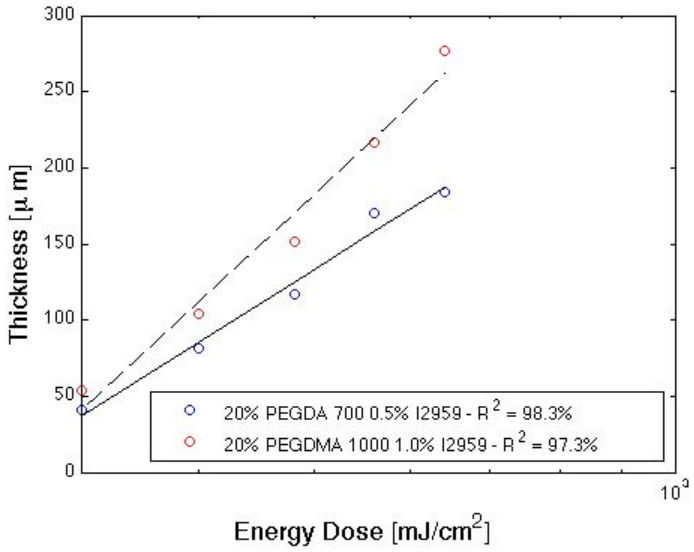

Figure 3.2: Characterization of cure depth as a function of ultraviolet energy dose

Dispersion of projected light through the pre-polymer solution results in an increase in the resolved feature size as the light penetrates further into the solution (Figure 3.3). Therefore, in order to preserve the small feature size patterning capabilities of the μSLA apparatus, a prescribed thickness of 50 μm was used for all x-y resolution characterization experiments. An increase in thickness will result in a corresponding increase in feature size.

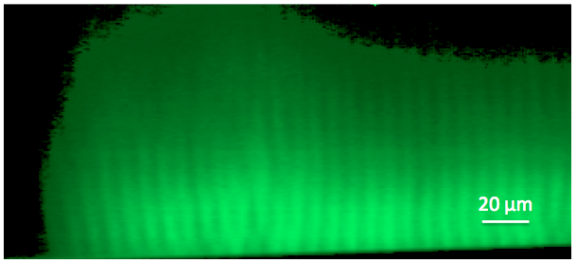

Figure 3.3: Resolved feature size decreases with increased penetration depth into pre-polymer solution, demonstrating the need for thickness control in the μSLA

Resolution characterization experiments of the smallest lines and holes that can be fabricated using the μSLA apparatus were conducted using PEGDA hydrogel polymers of molecular weight 700 g mol^{-1} and 1000 g mol^{-1}. Images of lines, holes, text, and other patterns were created using PowerPoint software and sent to the spatial light modulator (SLM), which

acted as a dynamic mask for polymerization, as described in Section 3.2.1. The shorter polymer chains in PEGDA 700 reduced swelling of the cured hydrogels, thereby resulting in higher resolution features (~ 2.5 µm) as compared to PEGDA 1000 hydrogels (~ 5 µm) (Figure 3.4).

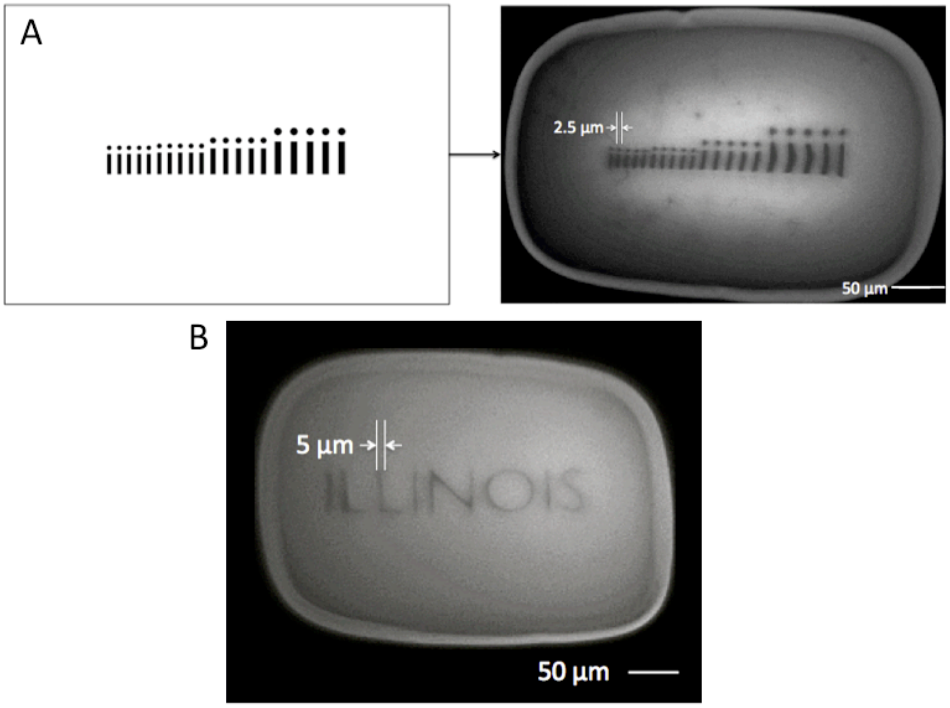

Figure 3.4: A) Demonstration of resolution with PEGDA 700 with dynamic SLM mask; **B)** Demonstration of resolution with PEGDA 1000 with dynamic SLM mask (50µm hydrogel thickness). Both PEGDA 700 and 1000 hydrogel polymers were mixed with Rhodamine B fluorescent dye prior to polymerization. Dark regions in fluorescent images indicate no polymer present, verifying that the high-resolution patterns are present throughout the gel thickness.

3.3.2 Fabrication of 3D Hydrogel Structures

Characterization of cure depth as a function of energy dose is useful for resolution studies, but is also an important factor in fabricating 3D hydrogel structures. The µSLA apparatus builds 3D structures through sequential layer-by-layer patterning of 2D cross-sections of a 3D design. In order for each new polymerized layer to bond to the previous layer, the ultraviolet light energy used to polymerize the current layer needs to penetrate into the previous layer, forming polymer chain cross-links between them. However, over-exposure of the previous layer to ultraviolet energy will result in over-curing of that layer, which has negative implications on the corresponding resolution that can be attained.

In this study, the first step in fabricating 3D hydrogel designs was determining the thickness of each layer of the structure. Using the characteristic equation of the μSLA apparatus, this thickness was translated into an appropriate energy dose. 2D cross-sections of a 3D design were created using PowerPoint software and sent to the spatial light modulator (SLM) sequentially, with the bottom-most layer appearing first. The first layer was chemically bonded to the micrometer stage via methacrylation and each subsequent layer bonded to the previous layer by the slight and well-characterized over-curing described previously.

PEGDA with different fluorescent markers was used to simulate fabrication with multiple materials (Figure 3.5). After polymerization of the first layer of the 3D structure, the remaining pre-polymer solution was washed away and replaced with a different pre-polymer solution to be used for the second layer. This demonstration of multi-material fabrication of structures is an important step in the quest to build 3D *in vitro* model tissues with different cell and biomaterial types.

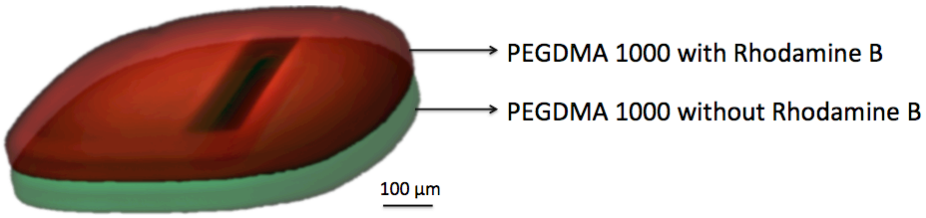

Figure 3.5: Fluorescence imaging of PEGDA 1000 hydrogel structures with and without Rhodamine B dye demonstrates the ability of the μSLA apparatus to fabricate multi-material 3D hydrogel structures, such as the hollow micro-channel shown here.

3.3.3 Cell encapsulation and viability

Encapsulating cells inside hydrogels using the μSLA apparatus introduces another component into the pre-polymer solution that causes dispersion of light, resulting in a reduced ability to resolve very small features. Furthermore, encapsulation of cells comes with the additional challenge of regulating light exposure. Over-exposure to ultraviolet light can damage and reduce the viability of cells encapsulated in the patterned hydrogels. While increasing the photoinitiator concentration can decrease the energy dose required to polymerize the hydrogels, the photoinitiator itself is cytotoxic in large doses and can reduce viability in the long term (Bryant 2012).

In this study, either NIH/3T3 fibroblasts or C2C12 murine myoblasts were suspended in PEGDA 1000 pre-polymer solution with 1.0% (w/v) photoinitiator (formulation described in Section 3.2.2) at concentrations ranging from 5E6 cells mL^{-1} to 20E6 cells mL^{-1}. Demonstration of feature sizes on the order of single cells was demonstrated using this pre-polymer formulation. MTS colorimetric assay was used to quantitatively assess for viability of encapsulated cells, as described in Section 3.2.5. Experiments showed that viability of encapsulated cells decreased with increasing energy dose (Figure 3.6). In long-term studies assessing viability at several time points, encapsulated cells were shown to remain viable within the hydrogel polymer matrix over a period of 7 days.

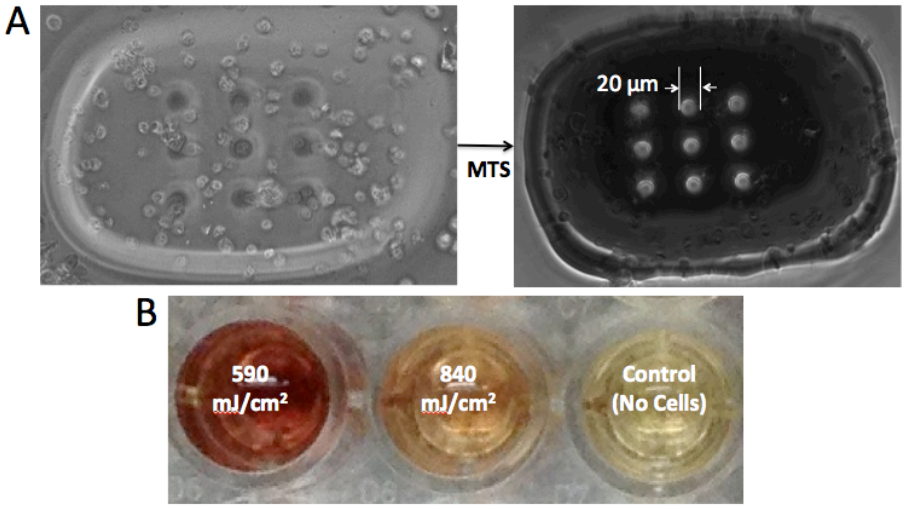

Figure 3.6: A) MTS Staining showing live C2C12 myoblasts encapsulated in PEGDA 1000 hydrogels with small-scale feature sizes (100 µm Thickness). Dark color post-MTS assay indicates the presence of living cells; **B)** Viability assessed via MTS for NIH/3T3 fibroblasts 72 hours after encapsulation in PEGDA 1000 hydrogels. Viability of encapsulated cells decreases with increasing energy dose.

3.4 DISCUSSION

The goal of building *in vitro* model biological systems for applications in programmable tissue engineering and the design of biological machines cannot be accomplished without enabling microfabrication technologies that allow for high resolution patterning of biomaterials, cells, and cell signals in three dimensions. The projection micro-stereolithography apparatus

presented in this study is capable of viably encapsulating cells in absorbent hydrogel polymers and patterning these structures at very high resolution.

As compared to other physical mask based polymerization apparatus, the dynamic mask technology enabled by the spatial light modulator in the μSLA allows for great flexibility in the design and fabrication of any 3D structure. Instead of directly tracing a design by rasterizing a laser, as is conventional in many existing stereolithographic bio-fabrication apparatus, the μSLA can polymerize whole patterns in one projection, without the need for rasterizing. This allows for high-throughput fabrication of large-scale structures with small feature sizes. While there have been other dynamic mask based projection stereolithography apparatus presented in the literature, these largely rely on digital micro-mirror devices (DMD) to act as dynamic masks for polymerization. These masks are limited in their ability to reproduce only black and white images, resulting in an "on" or "off" state for each pixel of the projected image (Sun 2005). By contrast, the use of a spatial light modulator (SLM) allows for projection of gray-scale images, allowing for smooth gradations of ultraviolet light energy projected onto the pre-polymer solution. This is anticipated to prove particularly advantageous for the fabrication of smoothly graded structures such as domes and spheres.

In this μSLA apparatus, the bottom layer is fabricated first and each subsequent layer is sequentially patterned and bonded to the previous layer to form the 3D structure. This bottoms-up "upside down" fabrication approach is novel and, in general, different from other projection stereolithography apparatus presented in the literature (Sun 2005, Zhang 2012). One advantage of this approach of fabricating parts is that it accommodates for cell-settling effects. In "right side up" approaches, prepolymer solution is dispensed on top of a fabricated layer prior to polymerization and cells start settling immediately. These systems are thus very sensitive to the time taken to polymerize parts and an even and controllable distribution of cells within the 3D structures is very difficult to accomplish. In the upside down approach, cells and prepolymer are directly dispensed into the prescribed volume of space between the polymerization stage and the micrometer stage immediately before hydrogel curing. This ensures that the cells are in fact evenly distributed throughout the multiple layers of the part. An additional advantage of the upside down approach for fabrication is that it readily enables incorporation of a dielectrophoresis (DEP) based cell patterning approach into the μSLA. Briefly, when electrodes are integrated with the polymerization stage of the apparatus and an electric field is generated,

cells align along the electrodes and can be aligned and patterned with high fidelity. While conventional approaches for incorporating DEP have only been able to pattern single layers of cells in hydrogels (Bajaj 2011), this upside down approach ensures that cells can be separately aligned and patterned in each layer. This also ensures that cells aren't exposed to the same fields multiple times, thereby increasing the viability of cells undergoing the encapsulation process. This integrated DEP system for highly precise and controllable patterning of cells is the future of this μSLA apparatus and shall be further discussed in Chapter 5.

3.5 CONCLUSION

A projection micro-stereolithography apparatus that uses a spatial light modulator as a dynamic mask for polymerization was designed and custom built for fabrication of 3D hydrogel structures with very small feature sizes, on the order of single cells. The relationship between energy dose and cure depth was well characterized and used to sequentially pattern and layer 2D cross sections of 3D multi-material designs. Feature size resolution of 2.5μm with PEGDA 700 and 5μm with PEGDA 1000 was demonstrated, along with the ability to preserve high resolution patterning with encapsulated cells in PEGDA 1000. Viability of cells encapsulated in hydrogels using the μSLA was quantitatively assessed as a function of ultraviolet energy dose and proven viable over a period of 7 days. The μSLA can thus be used to pattern cells and cell signals at high resolution for fundamental studies of cell mechanics and cell-matrix interactions. By enabling applications in tissue engineering, scaffold generation with living cells, and the development of biological machines, the μSLA will prove to be a promising enabling tool in the field of bionanotechnology.

CHAPTER 4: BIOLOGICAL MACHINES

4.1 INTRODUCTION

The emerging field of tissue engineering is centered on building complex biological substitutes for native tissue using a combination of cells and instructive biomaterials. While the goal of *reverse engineering* native tissue is promising for medical applications, it is not the only field of research opened up by work in this area. If we can rebuild existing systems with cells, we can also design novel systems that harness the innate dynamic abilities of cells to self-organize and respond to environmental cues. This idea of *forward engineering* integrated cellular systems with multiple functionalities is the core philosophy of engineering biological machines.

Perhaps the most intuitive demonstration of a biological machine is one that can generate force and produce motion. Cell-based soft robots, or "bio-bots," that can accomplish such objectives of robotics as sensing, storage and processing of signals, and a resultant response such as actuation can address many engineering challenges. A bio-bot can, for example, be engineered to detect a chemical toxin, achieve net motion towards it, and neutralize the toxin by releasing cell-secreted chemicals. This can be used to remove pathogens from water supplies or neutralize toxins *in vivo*. Recent studies have demonstrated bio-bots that use the autonomous and synchronous contraction of cardiac muscle cells as actuators for locomotion (Nawroth 2012, Chan 2012). While these machines demonstrate the power of using cells as building blocks for engineered systems, they are still quite primitive in that they lack the ability to be controlled via external signals.

In this study, a skeletal-muscle based biological machine was engineered and locomotion externally controlled via electrical and optical signals. The force production capabilities of these machines in the passive and active tension state of the muscle strip were characterized. Modeling and simulation of these machines was used to understand the effect of different design parameters on the machine, as well as to understand the mechanism of motion. Future generations of these microfabricated biological machines, including machines powered via the actuation of engineered cardiac muscle, are presented.

4.2 MATERIALS AND METHODS

4.2.1 MACRO-STEREOLITHOGRAPHY APPARATUS & PRE-POLYMER PREPARATION

A commercial laser-based stereolithography apparatus (SLA, Model 250/50, 3D Systems, Rock Hill, SC, USA) was custom-modified for building the bio-bots in this study. The SLA uses a HeCd gas laser as a source of 325 nm ultraviolet light. The laser beam is deflected by a set of scanning mirrors onto the polymerization stage of the SLA. Controlled scanning of the mirrors rasterizes the laser beam across the polymerization stage, allowing the apparatus to trace and cure hydrogels in specified 2D patterns at an x-y resolution of 250 μm (Figure 4.1).

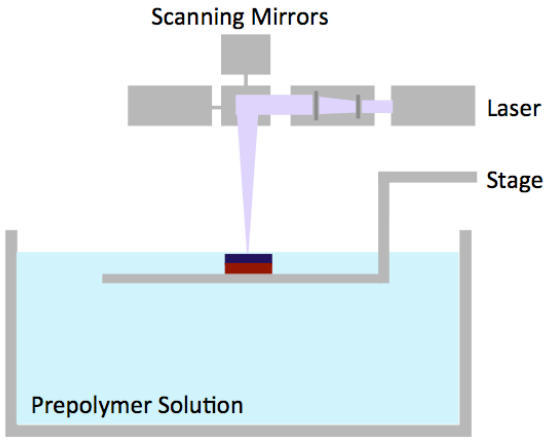

Figure 4.1: Schematic of laser-based stereolithography apparatus

3D designs for fabrication were generated using SolidWorks computer-aided design software (Dassault Systems, Velizy, France). Designs were converted into standard tessellation language (.stl) files and processed using 3DLightyear software (3D Systems, Valencia, CA, USA), which sliced the 3D designs into sequential 2D cross-sections. These cross-sections were processed by the SLA computer system and parts were fabricated layer-by-layer from the bottom up. Fabrication of 3D bio-bot and holder structures is detailed in Section 4.2.2.

Poly (ethylene glycol) diacrylate (PEGDA) hydrogels of molecular weight 700 g mol^{-1} and 1000 g mol^{-1} (Sigma-Aldrich, St Louis, MO, USA) were used to fabricate the bio-bots in this study. Prepolymer solutions of 20% (v/v) PEGDA 700 and 20% (w/v) PEGDA 1000 each with 0.5% (w/v) photoinitiator concentration were formulated as described in Section 3.2.2.

4.2.2 FABRICATION AND PROCESSING OF HYDROGEL BIO-BOT STRUCTURES

The 3D hydrogel bio-bot structure consists of two capped pillars connected by a flexible beam (Figure 4.2). The structure was fabricated as follows: First, a 18 mm square glass coverslip was taped to a 35 mm diameter dish and treated with oxygen plasma to render the surfaces hydrophilic. 1200 uL of PEGDA 700 prepolymer solution was pipetted onto the coverslip and the first layer of the bio-bot, the beam, was polymerized. Following this, the pillars and caps were fabricated in 200 μm thick layers with 250 uL of PEGDA 700 prepolymer solution per layer.

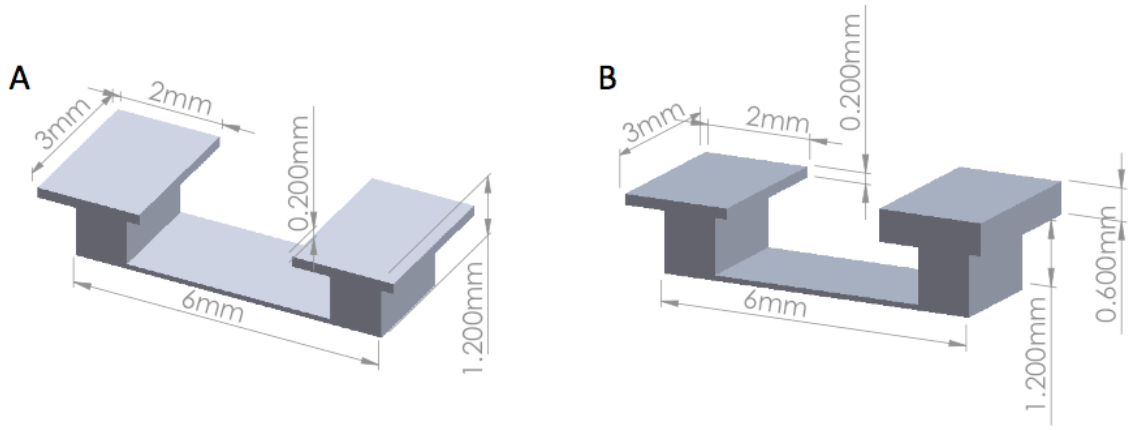

Figure 4.2: A) Symmetric bio-bot design; **B)** Asymmetric bio-bot design

To aid in the process of forming muscle strips, hydrogel holders for the bio-bot structures were fabricated using the SLA (Figure 4.3). The structure was fabricated as follows: First, an 18 mm square glass coverslip was methacrylated using the protocol detailed in Section 3.2.4 and taped to a hydrophilic dish. 1200 uL of PEGDA 1000 prepolymer solution was pipetted onto the coverslip and the first layer of the holder was polymerized, to correspond with the thickness of the first layer of the bio-bot beam. Following this, the walls of the holder were fabricated in 200 μm thick layers with 250 uL of PEGDA 1000 prepolymer solution per layer.

Immediately after fabrication, the hydrogel structures were washed in phosphate buffered saline (PBS, Lonza, Basel, Switzerland), sterilized in 70% ethanol (Decon Labs, King of Prussia, PA, USA) for 45 minutes, and stored in PBS at 4ºC until ready for cell seeding and muscle strip formation.

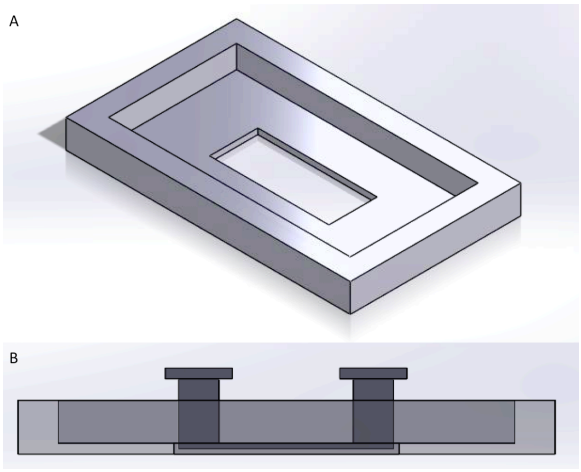

Figure 4.3: A) Holder design **B)** Holder and symmetric bio-bot final assembly.

4.2.3 MECHANICAL TESTING

Mechanical properties of the fabricated hydrogel structures were required for extraction of muscle force data as well as modeling and simulations. For this study, dogbone shaped tensile test specimens of the same material and thickness as the beam of the bio-bot were fabricated using the SLA. Beams of different stiffness were obtained by varying the ultraviolet energy dose of the SLA from 108.7 – 512.6 mJ cm^{-2}. Uniaxial tension was applied to the test specimens using a tensile test apparatus (ElectroForce Biodynamic 5100, Bose, Framingham, MA, USA) at a strain rate of 0.05 mm s^{-1}. Samples were maintained in an air-tight chamber filled with phosphate buffered saline throughout the testing process. A video extensometer was used to track the displacement of four marked points in the gauge section of the test specimen and control software was used to track the force exerted by the 100 g load cell and the corresponding strain in the specimen. Stress was computed by dividing the exerted force by the cross-sectional area of the specimen, as measured manually via calipers. Hooke's Law was used to compute the elastic modulus of the material from the linear region of the stress-strain curve.

4.2.4 CELL CULTURE

C2C12 murine myoblasts transfected with pAAV-Cag-Chr2-GFP-2A-Puro plasmin to express a light-sensitive ion channel, channel rhodopsin (ChR2), were used for the skeletal muscle bio-bots in this study (Sakar 2012). These cells were a gift from Professor Harry Asada at MIT. ChR2 C2C12s were maintained in growth medium: DMEM with 10% fetal bovine serum

(FBS, Sigma Aldrich, St Louis, MO, USA), 1% penicillin-streptomycin and 1% L-glutamine (Cellgro Mediatech, Herndon, VA, USA) in an incubator at 37ºC and 5% CO_2. Cells were regularly passaged 1:10 when they reached 70-80% confluency.

Primary ventricular cardiomyocytes used for cardiac muscle bio-bots in this study were isolated from neonatal (1-3 days old) Sprague-Dawley rats (Harlan Laboratories, Indianapolis, IN, USA) using a protocol approved by the Institutional Animal Care and Use Committee (IACUC Protocol #11160). Whole hearts were excised and placed in cold PBS. The atria and blood vessels were removed using small scissors and forceps and the remaining ventricles were quartered into 1-2 mm^2 pieces. The quartered hearts were digested in 0.05% (w/v) trypsin (TrypLE Express, Gibco, Carlsbad, CA, USA) in PBS for 16-18 hours on a shaker at 4°C. Trypsin digestion was halted by adding growth medium and the tissue fragments were transferred to a solution of 0.2% (w/v) type II collagenase in PBS for 45 minutes while shaking at 37°C. Mechanical trituration was used to release cells from the tissue fragments following collagenase incubation and the cell suspension was filtered through a 70 μm cell strainer (BD Biosciences, Franklin Lakes, NJ, USA) to remove undigested tissue. The filtered suspension was centrifuged at 750 rpm for 4 minutes and resuspended in growth medium. Cells were preplated in a tissue culture flask for one hour to enrich for cardiomyocytes and then either seeded in muscle strips or plated. Plated cells were maintained in growth medium: DMEM with 10% fetal bovine serum (FBS, Sigma Aldrich, St Louis, MO, USA), 1% penicillin-streptomycin and 1% L-glutamine (Cellgro Mediatech, Herndon, VA, USA) in an incubator at 37ºC and 5% CO_2.

HEK293 human embryonic kidney cells used for the cardiac muscle bio-bots in this study were transfected with pAAV-Cag-Chr2-GFP-2A-Puro plasmin to express a light-sensitive ion channel, channel rhodopsin (ChR2). HEK 293 cells were maintained in growth medium: DMEM with 10% fetal bovine serum (FBS, Sigma Aldrich, St Louis, MO, USA), 1% penicillin-streptomycin and 1% L-glutamine (Cellgro Mediatech, Herndon, VA, USA) in an incubator at 37ºC and 5% CO_2. Cells were regularly passaged 1:10 when they reached 70-80% confluency.

4.2.5 Formation of 3D muscle strips

To form the 3D muscle strips, the bio-bot hydrogel structures were placed in the holders. Cells were suspended in a gel solution of synthetic extracellular matrix and the solution was pipetted into the well of the holder. Over time, the traction forces exerted by the cells caused the

cell/gel solution to compact into a 3D muscle strip capable of contractility and force generation Muscle strips formed by cells seeded in a synthetic extracellular matrix composed of either fibrin or collagen were used in this study.

Formulation of fibrin cell/gel matrix solution: Cells were suspended in room temperature growth medium at a concentration of 5-10 E6 cells mL^{-1}. A stock 0.5U/mg solution of thrombin from bovine plasma (Sigma Aldrich, St Louis, MO, USA) was added to the cell suspension to make a 0.5% (v/v) concentration of the final cell/gel matrix solution. Matrigel basement membrane matrix (BD Biosciences, Franklin Lakes, NJ, USA) at 4ºC was added to the cell suspension at a concentration of 30% (v/v) of the final matrix solution. Finally, a 4mg/mL stock solution of fibrinogen (Sigma Aldrich, St Louis, MO, USA) at 4ºC was added to the cell suspension at a concentration of 50% (v/v) of the final matrix solution. The final cell/gel solution was pipetted into the well of a holder/bio-bot assembly and allowed to set at 37ºC for 45 minutes before the addition of warm growth medium.

Formulation of collagen cell/gel solution in room temperature growth medium at a concentration of 5-10 E6 cells mL^{-1}. Matrigel basement membrane matrix (BD Biosciences, Franklin Lakes, NJ, USA) at 4ºC was added to the cell suspension at a concentration of 10% (v/v) of the final matrix solution. A solution of collagen type I at 4ºC (BD Biosciences, Franklin Lakes, NJ, USA) was mixed with growth medium at a 1:1 volumetric ratio, forming a 76% (v/v) concentration of the final matrix solution. A solution of 0.1 M NaOH (Sigma Aldrich, St Louis, MO, USA) was added to this solution to form a 10% (v/v) concentration of final matrix solution. These two solutions were combined and seeded into the well of a holder/bio-bot assembly and allowed to set at 37ºC for 75 minutes before the addition of warm growth medium.

Both fibrin and collagen matrix bio-bots were preserved in an incubator at 37ºC and 5% CO_2 and media was replaced every 24 hours. The bio-bot structures deformed in response to the formation of the muscle strip and were removed from the holders on the second day. Cardiac bio-bots were maintained in growth medium throughout the study period. Skeletal muscle bio-bots were maintained in differentiation medium after the first day. This medium consisted of DMEM with 10% horse serum (Lonza, Basel, Switzerland), 1% penicillin-streptomycin, 1% L-glutamine (Cellgro Mediatech, Herndon, VA, USA), either 0 or 50 ng/mL human insultin-like

growth factor-1 (IGF-1, Sigma-Aldrich, St Louis, MO, USA) and either 1 or 2 mg/mL anti-fibrinolytic 6-aminocaproic acid (ACA, Sigma-Aldrich, St Louis, MO, USA).*

4.2.6 ELECTRICAL STIMULATION

Contractility of bio-bot muscle strips was triggered via electrical stimulation using a custom built apparatus (Bajaj 2011) (Figure 4.4). Prior to stimulation, bio-bots were transferred to a dish containing serum-free medium. The beam of the bio-bot lay parallel to a pair of platinum electrodes connected to the stimulation apparatus. Electrical square-wave signals of 20V amplitude and 50ms pulse width of frequencies from 1-3Hz were conveyed through the electrodes, driving contraction of the engineered muscle. Videos of stimulation were acquired with a digital microscope camera (FLEX, SPOT Imaging, Sterling Heights, Michigan, USA) at 10 fps.

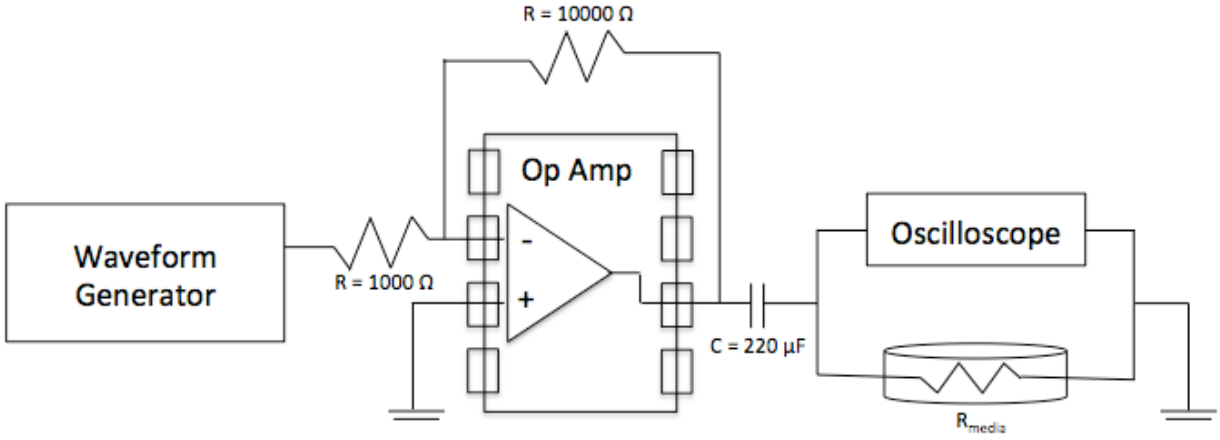

Figure 4.4: Schematic of electrical stimulation apparatus used to pace bio-bots.

4.2.7 OPTICAL STIMULATION

Contractility of bio-bot muscle trips was triggered via optical stimulation using an LED emitting blue light at a wavelength of 490 nm. The LED was connected to a function generator and square-wave signals of 10V amplitude and 100-200ms pulse width of frequencies from 1-3Hz were used to drive optically stimulated contraction of the engineered muscle. Top-view

* The bio-bot muscle strips characterized in the electrical pacing studies were fabricated and imaged by Caroline Cvetkovic, a student in Dr. Rashid Bashir's research group at the Univeristy of Illinois at Urbana-Champaign.

videos of stimulation were acquired using an inverted microscope (IX81, Olympus, Center Valley, PA, USA) and CCD camera (RT3, SPOT Imaging, Sterling Heights, Michigan, USA) at 12fps. Side-view videos of stimulation were acquired using a camcorder (Handycam DCR-SR65, Sony, Tokyo, Japan) at 30 fps.

4.2.8 TISSUE FIXATION

Bio-bot muscle strips were fixed in 4% formaldehyde (CAT RT 15710, EMS, Hatfield, PA, USA) for 30 minutes, washed in phosphate buffered saline (PBS, Lonza, Basel, Switzerland) for 15 minutes, and permeabilized in 0.2% (v/v) Triton X-100 in PBS (Sigma Aldrich, St Louis, MO, USA). Following this step, muscle strips were washed in PBS for fifteen minutes and preserved in signal Fx enhancer (I36933-IT, Invitrogen, Carlsbad, CA, USA) at 4ºC in preparation for immunostaining.

4.3 RESULTS

4.3.1 PASSIVE TENSION GENERATED BY ENGINEERED SKELETAL MUSCLE

Cells encapsulated in a synthetic extracellular matrix composed of fibrin exerted traction forces that compacted the cell/gel matrix solution over time into a 3D strip of engineered muscle. As the strip formed around the compliant microfabricated hydrogel structure, the two pillars of the bio-bot served as anchors for the muscle strip (Figure 4.5). The beam of the bio-bot underwent a change in conformation in response to the passive tension force generated by the engineered muscle. Since tensile force production is an important characteristic of the performance of engineered muscle, characterizing this force was a first step in assessing the functional behavior of these engineered bioactuators.

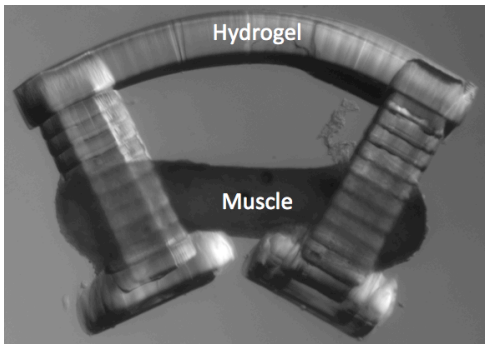

Figure 4.5: Cells seeded in a fibrin gel matrix exert traction forces to compact into an engineered muscle strip around 3D printed hydrogel bio-bot structure.

In this study, PEGDA 700 hydrogel bio-bot beams were polymerized using the SLA apparatus with ultraviolet light energy doses varying from 108.7 – 512.6 mJ cm^{-2}. Hydrogel test specimens were loaded in a tensile test apparatus and force-displacement data was recovered as described in Section 4.2.3. Since these hydrogels behave as linear elastic materials at low strain rates (Anseth 1996, Kloxin 2010), the elastic modulus was readily retrieved from the linear portion of the stress-strain curve as described by Hooke's Law, $\sigma = E\varepsilon$. Modulus of beams increased with increasing ultraviolet energy dose and varied from 214.6 – 741.6 kPa (n = 5, Figure 4.6).

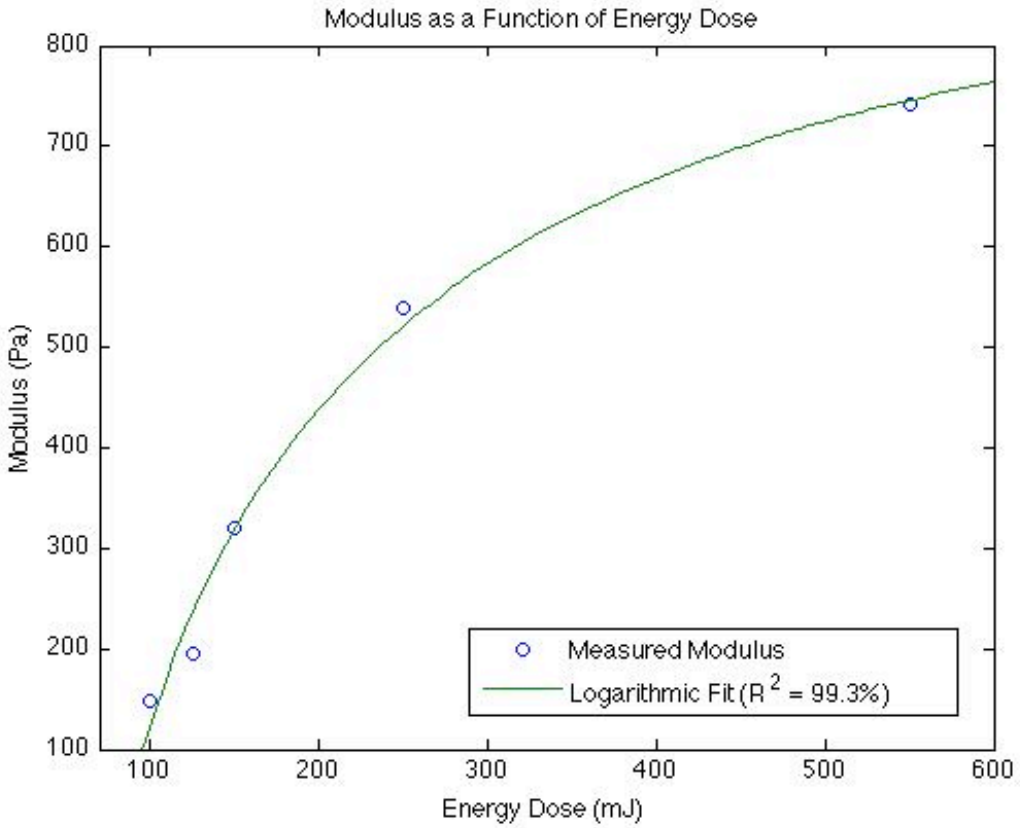

Figure 4.6: Modulus of polymerized hydrogels as a function of ultraviolet energy dose of SLA laser beam. A logarithmic fit provides an accurate description of this relationship.

Fibrin matrix muscle strips with skeletal muscle cells encapsulated at a concentration of 5E6 cells mL^{-1} were cultured in differentiation medium containing 50 ng/mL of human insulin-like growth factor, IGF-1, and 1 mg/mL of anti-fibrinolytic aminocaproic acid, ACA. Muscle strips were imaged over a period of nine days to observe the evolution of muscle strip formation

as a function of time and beam modulus. The maximum deflection of the center of the beam along with the distance of the muscle strip centroid from the beam was measured and recorded using ImageJ image analysis software (National Institutes of Health). As per Euler-Bernoulli beam theory, the differential equation that relates the deflection of a curved beam to the applied moment is given below:

$$\frac{-Pl}{EI} = \frac{d\theta}{ds} = \frac{y''}{\sqrt{1 - y'^2}}$$

In this equation, P is the passive tension generated by the muscle strip, y is the transverse deflection of the beam, l is the distance between the muscle strip and the beam (effectively the moment arm of the force), E is the elastic modulus of the deformed beam, and I is the moment of inertia of the beam.

Under the assumptions of small strain and small rotation (i.e. y' is considered negligible), the baseline tension, P, can be recovered as a function of the maximum deflection of the beam, δ_{max}, as follows:

$$\frac{d^2y}{dx^2} = \frac{M}{EI} \quad y(0) = 0, \quad y'\left(\frac{L}{2}\right) = 0$$

$$y = \frac{My^2}{2EI} - \frac{MLy}{2EI}$$

$$\delta_{max} = \left|y\left(\frac{L}{2}\right)\right| = \frac{ML^2}{8EI}$$

$$M = Pl = \frac{8EI\delta_{max}}{L^2}$$

$$P = \frac{8EI\delta_{max}}{lL^2}$$

Using the known geometric and material properties of the hydrogel beam, as well as the measured deflection of the beam and moment arm of the muscle strip, passive tension force was recovered for bio-bots with hydrogel beams of varying stiffness. For moduli of 214.6, 319.4, 411.2, and 489.3 kPa, the passive tension recorded over days 2-9 averaged 860.6 ± 47.2, 992.7 ± 34.3, 1103.6 ± 45.8, and 1146.0 ± 69.0 μN respectively. There is a positive correlation between increasing beam stiffness and increasing passive tension in the muscle (Figure 4.7).

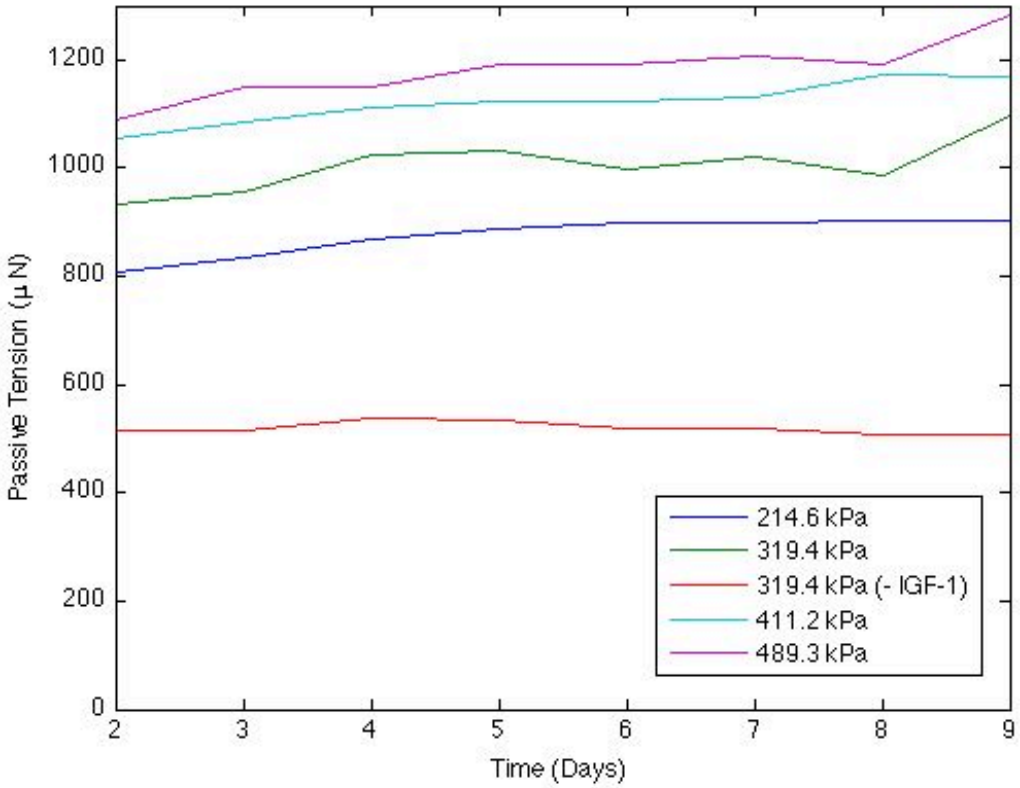

Figure 4.7: Passive tension force generated by engineered muscle strip increases for increasing bio-bot beam moduli. Passive tension force is dependent on the presence of IGF-1.

To compare the force generated by these muscle strips to other engineered muscle systems, the passive stress in the tissue was calculated by dividing tension by the measured cross-sectional area of the muscle strips, 1.19 ± 0.04 mm^2 as determined by transverse histological cross-sections. On average, the passive stress averaged 0.84 ± 0.03 kPa, falling within the range of stress values reported in the literature for similar engineered systems of different scales, but significantly lower than the force produced by native muscle (260 kPa) (Lam 2009).

Passive tension was studied as a function of various parameters such as concentration of IGF-1 in the differentiation medium, concentration of ACA in the differentiation medium, and concentration of cells in the cell/gel matrix solution. Fibrin based muscle strips of beam stiffness 319.4 kPa, with cells encapsulated at 5E6 cells mL^{-1} and cultured without IGF-1 developed a lower passive tension force of 581.4 ± 20.4 μN, on average. This is a 41.4% decrease in force

production as compared to the muscle strips cultured with 50ng/mL IGF-1. Similarly, fibrin based muscle strips of beam stiffness 319.4 kPa cultured with 2 mg/mL ACA demonstrated an 11.6% decrease in force production as compared to the muscle strips cultured with 1 mg/mL ACA.

Fibrin matrix muscle strips with skeletal muscle cells encapsulated at a higher cell concentration of 10E6 cells mL^{-1} demonstrated a corresponding increase in passive tension force to 1236.18 ± 49.2 μN, a 24.5% increase in tension as compared to the muscle strips with 5E6 cells mL^{-1}. These dependencies of passive tension force on the cell/matrix composition and culture conditions as well as the modulus of the hydrogel bio-bot structure illustrate the dynamic modeling capabilities of engineered skeletal muscle.

To verify the accuracy of the passive tension values extracted using Euler-Bernoulli beam theory, the computed force values were input to the bio-bot structure in an ANSYS based finite element simulation (ANSYS, Canonsburg, PA, USA). The resulting deflections of the simulated beams of stiffness 214.6, 319.4, and 489.3 kPa were 1.24, 1.004, and 0.44 mm respectively (Figure 4.8). These values decreased with increasing material stiffness, as expected, since these materials offered greater resistance to the bending motion produced by the cell traction forces. Simulated deflection values differed by approximately 18%, on average from the experimentally measured deflection values on Day 8 of culture, indicating that the linear bending theory model provides a sufficiently accurate prediction of the force produced in the engineered muscle strip.

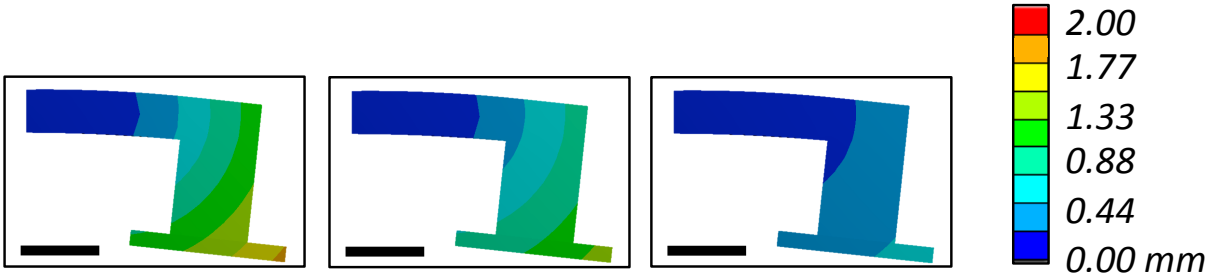

Figure 4.8: Finite Element Analysis of beam deflection as a function of bio-bot beam stiffness. Increased stiffness offers a greater resistance to bending and therefore a smaller deflection.

4.3.2 ACTIVE TENSION GENERATED BY ENGINEERED SKELETAL MUSCLE

Stimulation by electrical or optical signals causes contraction of the engineered muscle strip. The resulting increase in tension, as compared to the baseline passive tension, is termed the active tension generated by the muscle. Treating the hydrogel bio-bot structure as a linear elastic material governed by Hooke's law, as before, the force, *F*, required to deform the beam by an amount *dx* is given by $F = kdx$, where *k* represents the stiffness of the structure. This stiffness was calculated by comparisons of the un-deformed and deformed, or passive tension, state of the bio-bot structure:

$$k = \frac{P}{x_{undeformed} - x_{deformed}}$$

The amount of force required to the passive state is the passive tension force, *P*, calculated via Euler-Bernoulli beam theory, as discussed in Section 4.3.2.

An automated tracking script written in Matlab (MathWorks, Natick, MA, USA) based on a normalized 2D cross-correlation of successive frames in a video was used to extract the time varying distance between the two ends of a bio-bot during stimulation-induced contraction[†]. In these videos, the bio-bots were placed in a dish containing warm media and stimulated electrically, as described in Section 4.2.6. Knowing the stiffness, *k*, of the bio-bot structure as well as the passive tension force, *P*, the active tension force, *F*, generated by the contracting engineered muscle was calculated as follows:

$$F = P + \frac{P\ dx}{x_{undeformed} - x_{deformed}}$$

Fibrin matrix muscle strips with skeletal muscle cells encapsulated at a concentration of 5E6 cells mL^{-1} cultured in differentiation medium containing 50 ng/mL of IGF-1 and 1 mg/mL of ACA were seeded around both "symmetric" and "asymmetric" bio-bot structures, stimulated electrically, and paced at frequencies of 1,2, and 4 Hz as described in Section 4.2.6. As the

[†] Automated tracking script was written by Brian Williams, a graduate student in Professor Taher Saif's research group at the University of Illinois at Urbana-Champaign.

frequency of stimulation increased from 1 to 4 Hz, the magnitude of active tension forces above baseline passive tension decreased from 198.68 μN to 109.48 μN. Above a frequency of 8 Hz, tetanus of the muscle strip was observed. Muscle strips cultured in differentiation medium without IGF demonstrated no contractile behavior in response to electrical stimulation.

4.3.3 ELECTRICALLY STIMULATED LOCOMOTION OF SKELETAL MUSCLE BIO-BOT

Demonstration of external control-driven locomotion is the first step toward engineering bio-bots with complex functionality. In this experiment, bio-bots were placed in a dish containing warm media parallel to the electrodes in the stimulation apparatus and allowed to move freely across the surface of the dish. The electrical stimulation driven contraction of the muscle strip caused a change in conformation of the hydrogel beam. The resultant flexion caused the bio-bots to "crawl" across the substrate, demonstrating net locomotion.

Both symmetric and asymmetric bio-bots of beam stiffness 319.4 kPa were seeded with a fibrin matrix cell/gel solution containing 5E6 cells mL^{-1} and differentiated in culture medium with IGF and ACA. The bio-bots were electrically stimulated 7-13 days after seeding and demonstrated a range of velocities ranging from 0.66 – 69.5 μm s^{-1}. An average velocity of 13.4 ± 20.6 μm s^{-1} for symmetric bio-bots and 28.1 ± 25.2 μm s^{-1} for asymmetric bio-bots was observed[‡].

A representative bio-bot of both the symmetric and asymmetric bio-bot designs was chosen for analysis of locomotion in response to electrically paced contraction. Active tension was computed and a maximum active tension force of 73.76 μN above baseline passive tension for symmetric bio-bots and 787.93 μN above baseline passive tension for asymmetric bio-bots was recorded during electrical stimulation (Figure 4.9).

[‡] Velocity for electrically paced skeletal muscle bio-bots was calculated by Caroline Cvetkovic, graduate student in Dr. Rashid Bashir's research group at the University of Illinois at Urbana-Champaign.

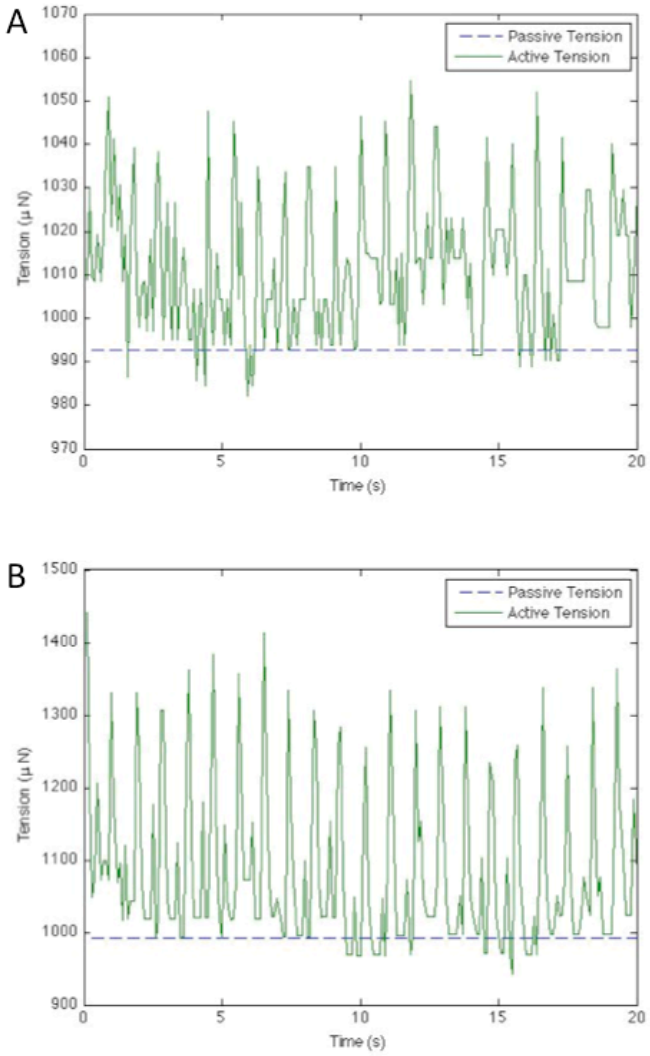

Figure 4.9: Active Tension of representative **A)** symmetric and **B)** asymmetric bio-bot designs paced via electrical stimulation at 1Hz frequency

4.3.4 MECHANISM OF LOCOMOTION OF SKELETAL MUSCLE BIO-BOT

Understanding the mechanism of locomotion of the skeletal muscle bio-bot is an important step in designing bio-bots with increased efficiency and functionality. A digital model of the bio-bot structure in its deformed passive tension state was generated using SolidWorks CAD software (Dassault Systems, Velizy, France) and imported into the ANSYS finite element package (ANSYS, Canonsburg, PA, USA). In order to recapitulate the walking motion captured in videos of electrically stimulated bio-bots, the tracked displacement of the right and left pillars of the bio-bot was input to the simulation. The bio-bots were placed on a frictionless support, or

"ground", and allowed to deform and move with respect to the ground in response to the displacement input. The simulation then output the time-varying stresses in the bio-bot structure as well as the time varying reaction force from the ground. These time-varying reaction forces were analyzed in order to understand the structure's mechanism of motion (Figures 4.10, 4.11).

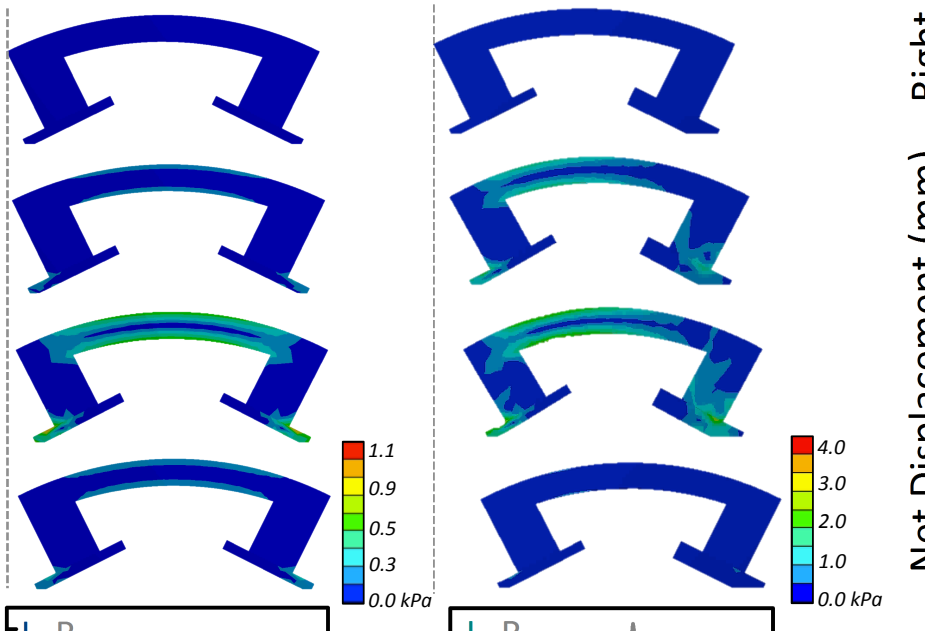

Figure 4.10: Electrically stimulated locomotion of representative symmetric and asymmetric bio-bot over a period of 10 seconds (1Hz stimulation frequency). The asymmetric bio-bot demonstrated greater displacement in response to electrical stimulation.

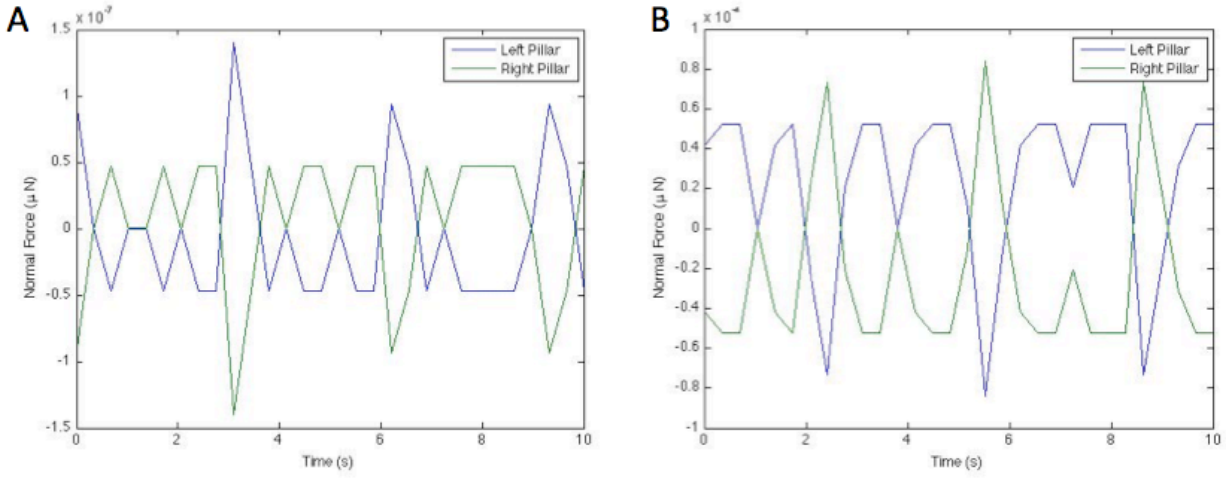

Figure 4.11: Reaction forces on representative **A)** symmetric and **B)** asymmetric bio-bots from ground during electrically stimulated actuation of bioactuators

To explain the bio-bot mechanism of motion, two phenomena and their significance in locomotive behavior were considered: 1) The range of motion experienced by the left and right pillars of the bio-bot, 2) the phase delay between the contractile response and time-varying coefficients of friction in the left and right pillars of the bio-bot. A combination of these two phenomena was used to describe the various types of locomotion observed in the bio-bots. For the representative samples of symmetric and asymmetric bio-bots considered in detail in this study, the active tension analysis and simulations of walking motion led to an improved understanding of the mechanism of locomotion.

The symmetric bio-bot demonstrated net locomotion in the direction opposite to the pillar with a greater range of locomotion (L/R > 1). In this case, the phase-delayed contraction caused the left pillar to initially remain static with respect to the ground while the right pillar slipped, followed by sliding of the left pillar towards the right. This was termed a "pushing" mechanism of locomotion. The asymmetric bio-bot demonstrated net locomotion in the same direction as the pillar with a greater range of locomotion (L/R > 1). In this case, the phase-delayed contraction caused the right pillar to initially remain static with respect to the ground while the left pillar slipped, followed by sliding of the right pillar in the direction of motion. This was termed a "pulling" mechanism of locomotion. All the bio-bots considered in this study were described by either this pushing or pulling mechanism of locomotion (Figure 4.12).

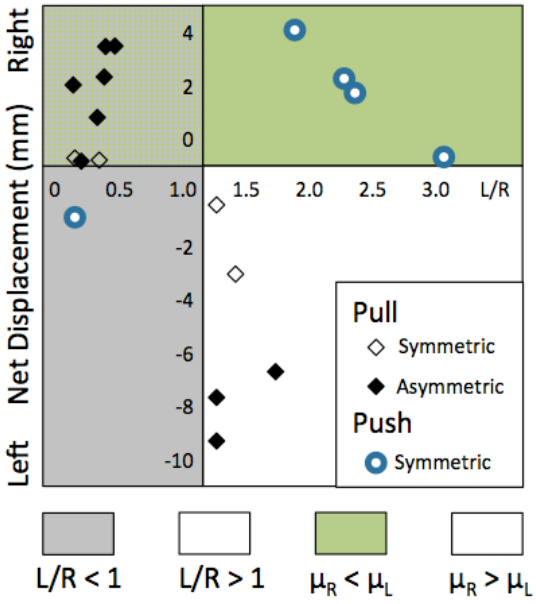

Figure 4.12: Schematic of mechanism of locomotion of all electrically paced symmetric and asymmetric skeletal muscle bio-bots stimulated during this study.

4.3.5 OPTOGENETIC SKELETAL MUSCLE BIO-BOT

Optogenetic skeletal muscle cells which have been genetically engineered to express a light-activated cation channel, Channelrhodopsin-2, contract in response to pulsed blue (490 nm) light, enabling targeted and noninvasive muscle actuation in real time.

In this study, optogenetic skeletal muscle cells were plated in a dish as a 2D monolayer and cultured in differentiation media containing 50 ng/mL IGF over a period of two weeks. The cells had formed mature myotubes by Day 6 of culture and demonstrated paced contractile response to optical stimulation at different frequencies on Day 8 of culture.

Based on these results, it was hypothesized that fibrin and collagen based bio-bots containing optogenetic skeletal muscle cells would form light-responsive myotubes that contract in response to pulsed blue light and demonstrate net locomotion in response to optical stimulation. A few representative cases of these optogenetic skeletal muscle bio-bots were engineered and analyzed in a similar fashion to the electrically paced skeletal muscle bio-bots discussed in the preceding sections.

On average, optogenetic bio-bots with beam stiffness of 319.4 kPa generated passive tension forces similar to those seen in prior studies for both collagen and fibrin based muscle strips. However, collagen-based muscle strips were observed to be less robust and snapped before Day 12 of culture. Fibrin-based muscle strips seeded around symmetric bio-bots demonstrated maximum dynamic active tension forces of 12.34, 13.65, 10.49, and 9.44 μN in response to optical stimulation of 1, 2, 3, and 4 Hz stimulation respectively. This force-frequency relationship is similar to that observed in electrical stimulation of muscle strips, as discussed in Section 4.3.2.

Individual bio-bots were stimulated both electrically and optically to generate a comparison of the active tension force generated in response to differing types of stimulation. These studies revealed that bio-bots generated the same active tension responses in response to both types of signaling, indicating that the force-generating capacity of optically stimulated bio-bots is functionally comparable to electrically stimulated bio-bots (Figure 4.13). Of the symmetric bio-bots that demonstrated net locomotion in response to optical stimulation, a maximum velocity of 5 μm s^{-1} was observed. It is anticipated that introducing asymmetry into the bio-bot structure, as discussed in the Section 4.3.3, will result in greater net displacement.

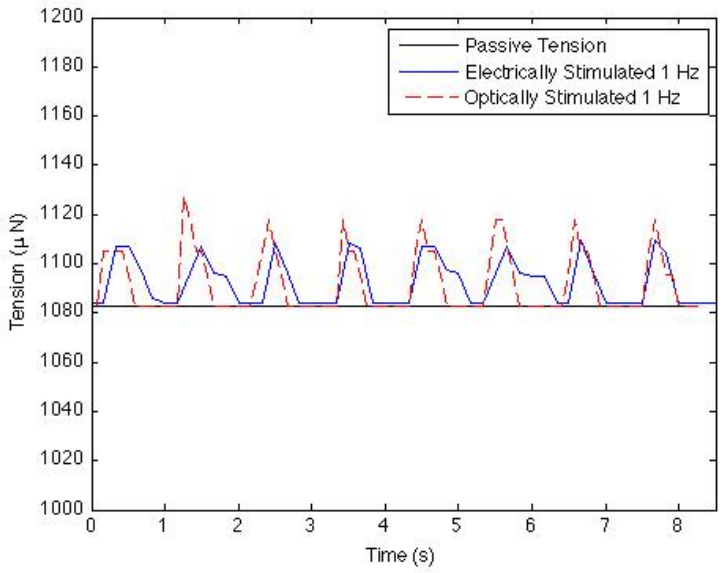

Figure 4.13: Optically stimulated contraction of engineered skeletal muscle yields active tension values that are comparable with electrically stimulated contraction of the same muscle strip.

4.3.6 OPTOGENETIC CARDIAC MUSCLE BIO-BOT

Optogenetic human embryonic kidney cells (HEK293T) that have been transfected to express Channelrhodopsin-2 (ChR2) were co-cultured with neonatal rat ventricular cardiomyocytes extracted as described in Section 4.2.4. It was hypothesized that the transfected kidney cells would form electrical gap junctions via the Connexin-43 protein when co-cultured with primary cardiomyocytes, triggering light-activated action potentials across the engineered cardiac muscle. Response of the co-culture system to optical stimulation was observed in 2D, where the cardiac and HEK cells were seeded on a poly (ethylene glycol) cantilever and optical stimulation was used to drive contraction of the engineered muscle tissue.

Based on this preliminary study, collagen-based 3D muscle strips with a co-culture containing 90% cardiomyocytes and 10% ChR2 HEK293T cells were seeded around hydrogel bio-bot structures with a beam stiffness of 319.4 kPa. The cardiac muscle formed highly compacted strips, but did not generate sufficient passive tension force to significantly deform of the compliant hydrogel beam (Figure 4.14). Electrical stimulation of these muscle strips resulted in observable local contractile response to cells, but not enough macro-scale contractile response of the tissue to result in significant deformation of the hydrogel beam. No net locomotion was observed.

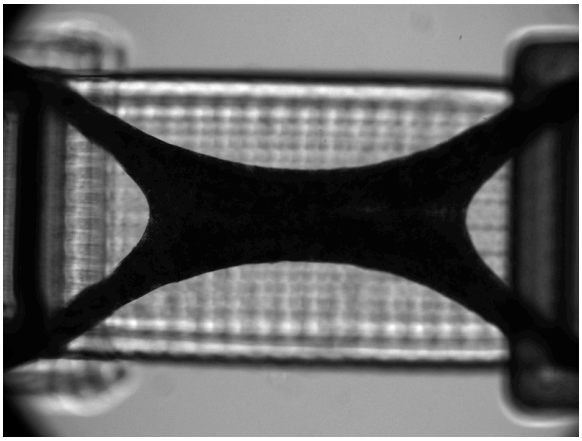

Figure 4.14: Collagen-based 3D cardiac muscle strips contain viable cells that respond to electrical stimulation signals. Macro-scale force generation and contractility was not observed.

4.4 DISCUSSION

The goal of building biological machines, or bio-bots, capable of demonstrating net locomotion in response to external signals has myriad applications including drug delivery, non-invasive surgery, and biocompatible microelectronic devices. The skeletal and cardiac muscle bio-bots presented in this study are capable of contractility and force generation in response to electrical and optical external signals. The flexion of the microfabricated soft hydrogel structure in response to contraction of the engineered muscle resulted in net locomotion of bio-bots across a substrate.

4.4.1 FORCE GENERATION AND CONTRACTILITY OF SKELETAL MUSCLE BIO-BOTS

Microfabrication via 3D printing is a novel technique that allows for great flexibility and scalability in the design of biological machines. In this study, a stereolithography apparatus was used to polymerize hydrogel structures of precisely defined geometric and material properties. The traction forces of cells seeded in a synthetic extracellular matrix caused the hydrogel beam of the bio-bot to deform into a passive tension state. This passive tension force generated by engineered muscle was computed as a function of the stiffness of the hydrogel beam and a positive correlation between increasing beam stiffness and increasing passive tension was observed. This indicated that engineered muscle differentiated in a higher stiffness environment generates more passive tension force over time, an observation that agrees with the observation

that mechanical stimulation has been proven to improve the performance engineered skeletal muscle (Powell 2002). Experiments on the effect of human insulin-like growth factor, IGF-1, on passive tension were conducted and observed to cause an increase in the force generated by the engineered muscle. While incorporation of anti-fibrinolytic agents such as aminocaproic acid (ACA) into the differentiation medium improved the mechanical integrity and long-term stability of the muscle strip, an increase in ACA concentration led to a decrease in passive tension force generated by the muscle strip. Similarly, an increase in the cell concentration caused an increase in passive tension force, corresponding to the greater number of myotubes formed in the engineered muscle strip. This is an interesting and novel advantage of biological machines over conventional systems, as the dynamic response and evolution of living cells and components allows for a greater variety of functional responses.

Both electrical and optical signals were used to stimulate contraction of engineered skeletal muscle and the resultant active tension behavior were observed in bio-bots cultured in differentiation medium cultured with IGF-1. The magnitude of active tension forces above baseline passive tension was shown to decrease with increasing frequency of stimulation. This observation seemed to contradict the physiological behavior of skeletal muscle, which demonstrates an increase in force generation with increasing frequency of contraction before reaching tetanus. However, the force-frequency relationship observed in the bio-bots can be attributed to the viscoelastic behavior of the hydrogel structure that, while behaving as a linear elastic material at low strain rates, demonstrates rate-dependent material properties at higher strain rates (Anseth 1996). At higher frequencies, there is a greater resistance to deformation of the hydrogel structure and hence, it is possible that the active tension force does in fact increase with increasing frequency of stimulation. Further work on this platform will include models and simulations that more rigorously address the viscoelastic response of the hydrogel structures used in these studies.

4.4.2 LOCOMOTIVE RESPONSE OF SKELETAL MUSCLE BIO-BOTS

A range of locomotive responses was observed in bio-bots with both symmetric and asymmetric geometric designs. On average, the controlled asymmetry of design led to more readily controllable directional movement and an increase in the functional performance and average velocity of the biological machine.

In the bio-bot structures, one pillar generally experienced a greater range of motion than the other. The range of motion was determined by two factors: beam curvature and normal force from the ground. Beam curvature was dependent on both the force in the muscle strip and the moment arm between the muscle strip and the beam. Since both pillars were attached to the same muscle strip, the force exerted on each pillar was the same. However, differences in cell/gel compaction led to different moment arms in the left and right pillars, causing in greater bending on one side of the beam and hence greater pillar displacement on the corresponding side. This was more apparent in the asymmetric bio-bot structures, as the increased length of one pillar generally corresponded to an increase in the moment arm of the muscle strip attached to that pillar. The normal force from the ground regulated the frictional force, which in in turn regulated the displacement of the pillar. As the bio-bot deformed and walked in response to electrical stimulation, the asymmetric distribution of mass in the muscle strip shifted and the weight borne by each pillar varied as a function of time. This caused a time varying normal force reaction response from the ground, and hence a time varying friction force on the pillars. A combination of these two factors determined which pillar experienced a greater range of motion.

In the bio-bot structures, directional motion occurred when differential coefficients of friction between the left and right legs caused one leg to “stick” and the other to “slide” with respect to the ground. This differential coefficient of friction between the legs was a result of a phase delay between the contractile response of the left and right legs in response to electrical stimulation. This phase delay was attributed to the fact that macro-scale contractile response is a sum of multiple micro-scale local responses of myotubes responding to electrical stimulation. The summed contractile response of individual myotubes distributed throughout the muscle strip determined the structure-wide response.

As discussed in section 4.3.4, the asymmetric design led to a greater difference in range of motion of the different pillars of the bio-bot as well as a greater discrepancy in the time-varying coefficients of friction of the bio-bot pillars. These factors led to a greater functional locomotive response, on average, in the asymmetric bio-bots.

4.4.3 OPTOGENETIC CONTROL OF SKELETAL AND CARDIAC MUSCLE BIO-BOTS

Optogenetic control of engineered muscle based biological machines allows for non-invasive external signaling to drive locomotion of bio-bots. In this experiment, methods for controlling both skeletal and cardiac muscle based bio-bots were explored and characterized.

Optogenetic skeletal muscle cells transfected to express a light sensitive ion channel, Channelrhodopsin-2, were incorporated into the 3D fibrin and collagen based muscle strips developed in the electrical stimulation portion of the study. These muscle strips showed a similar ability to generate force and demonstrate contractile behavior in response to both electrical and optical signals. On average, the maximum magnitude of active tension force generated by optical stimulation of the optogenetic skeletal muscle symmetric bio-bots at 1 Hz was 12.34 μN. The bio-bots demonstrated similar functional responses to optical stimulation as compared to electrical stimulation. The maximum velocity demonstrated by optically stimulated symmetric bio-bots was 5 μm s^{-1}, a value which falls within the range of velocities demonstrated by symmetric bio-bots stimulated via electrical pacing.

The low yield and inability to repetitively use primary cardiomyocytes that have undergone direct transfection to express light-sensitive ion channels made this an inefficient method for producing optogenetic cardiac muscle based bio-bots. To that end, a simpler and more efficient method for was developed by transfecting human embryonic kidney cells to express ChR2 and co-culturing these cells with cardiomyocytes to form electrical gap junctions via the Connexin-43 protein (McSpadden 2009). In this study, optogenetic HEK293T cells were co-cultured with primary cardiomyocytes and the electrical coupling between these two cell types in the engineered cardiac muscle tissue was shown to display contractile response to optical stimuli. However, 3D muscle strips containing similar co-culture of cells only displaced local response to stimulation, with no macro-scale contraction of the tissue and resultant locomotion of the bio-bot structure. This was attributed to the fact that viability of primary cardiomyocytes following the extraction procedure is generally low. When these co-cultures are plated in a substrate in 2D, the dead cells are washed away and only living cells survive and proliferate across the substrate, generative action potentials that traverse the entire cell sheet and are paced by optical stimuli. By contrast, in 3D muscle strips, the dead cells are trapped within the muscle strip and decrease the cell to matrix ratio of the engineered muscle. This results in a decreased ability to generate macro-scale contractile force. Further optimization of the extraction

and seeding protocol is expected to improve the response of optogenetic cardiac muscle bio-bots to optical signals. It is anticipated that the high cell density resulting from tissue compaction into a 3D strip will result in more efficient force production, as compared to a 2D cell sheet on a substrate.

4.5 CONCLUSION

Tissue engineering has introduced a new set of materials into the human toolbox: living cells and biological signals. This enables an array of exciting new technologies. The dynamic nature of living components to perform myriad sensing and actuation tasks can be harnessed to forward engineer biological machines. In this study, skeletal and cardiac muscle based bio-bots were engineered to generate force and produce motion in response to external stimuli. Novel methods of measuring the contractile force generated by the engineered muscle were generated and executed. The mechanism of motion of skeletal-muscle based bio-bots in response to electrical pacing was characterized using a finite element analysis solution.

Genetic modification was used to transfect mammalian cells with light-gated ion channels that allow for the high specificity and spatiotemporal resolution of optical stimulation, as compared to electrical signaling. This optical stimulation was used to drive locomotion of skeletal muscle based bio-bots and shown to result in contractile behavior of cardiac muscle based bio-bots. The bio-bots engineered in this study promise to establish a basis for the design rules and principles that govern building biological machines that can sense external signals, process them, and demonstrate a controlled locomotive response to them. Bio-bots that can dynamically respond to environmental cues in this manner have a wide array of applications, including human health.

CHAPTER 5: CONCLUSION AND FUTURE DIRECTIONS

5.1 PROJECTION MICRO-STEREOLITHOGRAPHY APPARATUS

Microfabrication via 3D printing is a novel technique that allows for flexibility and scalability of design with precisely defined geometric and material properties. In this study, a stereolithographic apparatus was used to pattern highly porous and absorbent poly (ethylene glycol) hydrogels at very high resolution, on the order of single cells in the body. These hydrogels promoted the viability and proliferation of encapsulated cells and promise to provide an integrative platform for engineering *in vitro* substitutes for native tissue and organs.

5.1.1 INTEGRATED DEP-μSLA SYSTEM

In the current μSLA, cells are mixed in a pre-polymer solution and assumed to distribute evenly throughout the solution. As the projected light polymerizes patterns in the pre-polymer, cells are encapsulated immediately with no further control of patterning. Since the feature sizes being patterned are on the order of single cells, a cell positioned in an improper location can reduce the fidelity of high-resolution patterning with this apparatus. Researchers have demonstrated the ability to control the positioning of live cells in patterned hydrogels using patterning (Hynd 2007, Chan 2012), optical trapping of live cells followed by encapsulation in photopolymerizable hydrogels (Chiou 2005, Mirsaidov 2008, Linnenberger 2013), dielectrophoretic control of live cells followed by encapsulation in photopolymerizable hydrogels (Fan 2008, Bajaj 2012), and even magnetic cell levitation in 3D hydrogel tissue culture systems (Souza 2010). While these techniques are promising, they come with many challenges and disadvantages. For example, optical trapping requires the use of multiple optical tweezers to organize cells into complex arrays prior to encapsulation in photosensitive polymeric hydrogels. While this technique allows for precise patterning of cells in hydrogels, it is limited by the number of cells that can be trapped at a time and requires specifying the position of individual cells, a degree of precision that is not often necessary.

Dielectrophoresis (DEP) based approaches for precision patterning of cells allow for a more efficient approach to manipulating and patterning cells. In this approach, cells align along specified directional patterns in response to the electrical fields generated by patterned

electrodes. This technique enables the formation of precisely defined cellular patterns in a much more high-throughput and parallel process than allowed by optical trapping or similar single-cell based approaches. For this reason, it is anticipated that the projection micro-stereolithography apparatus, μSLA, described in Chapter 3 can be further improved by incorporating DEP electrodes into the platform of the polymerization stage (Figure 5.1).

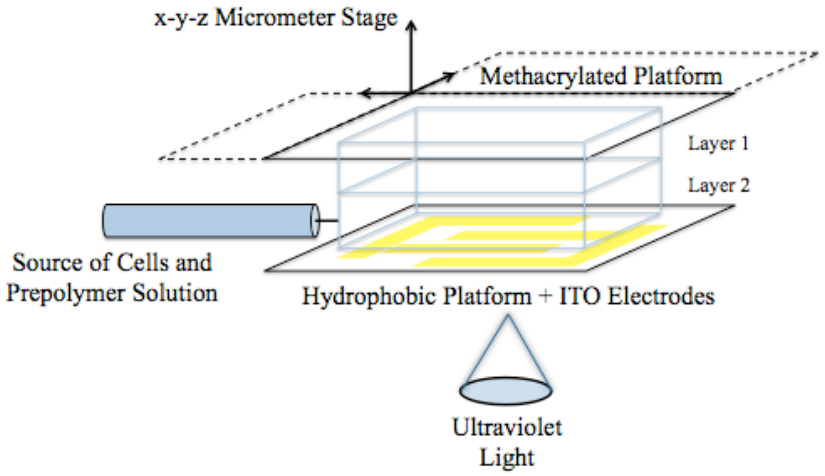

Figure 5.1: Schematic of integrated DEP- μSLA system

As the prepolymer-solution containing cells is pipetted onto the hydrophobic polymerization stage of the μSLA, the electric fields generated by the transparent Indium tin oxide (ITO) electrodes will align and pattern the cells. Once the cells are aligned, they will be trapped in place by the ultraviolet light energy induced polymerization of the pattern generated by the spatial light modulator (SLM). The methacrylated micrometer stage will move up, allowing for similar patterning and encapsulation of cells in subsequent layers of the 3D design. This approach, in addition to allowing patterning of cells in 3D in a massively parallel fashion, also avoids exposure of the encapsulated cells to multiple electrical and optical field exposures, preserving long term viability. The engineered tissues that can be created this system will have micro-scale feature sizes and precisely defined morphological and functional properties in 3D, extending the applications of this technology to realms not previously possible in bionanotechnology.

5.1.2 APPLICATIONS OF μSLA SYSTEM

Applications of the μSLA extend far beyond the scope of the studies covered in this document. Previous studies with the macro-scale SLA have demonstrated the ability of fibroblasts encapsulated in hydrogel micro-well "patches" to secrete angiogenic factors and pattern blood vessels *in vitro* (Jeong 2012). These patches are limited in their ability to generate a high flux of angiogenic factors because the microwell diameter cannot be decreased with the current SLA apparatus without exceeding the resolution limits of the system. The μSLA can, however, pattern patches with much smaller feature sizes than capable with the SLA. Future studies of such microfabricated patches implanted *in vivo* can, therefore, could lead to the generation of high fidelity perfusable vascular networks.

The μSLA was built as a replacement for the existing macro-scale SLA apparatus that was used to fabricate the bio-bots used in this study. Future generations of bio-bots that target *in vivo* applications will need to be scaled down in order to traverse the microvasculature of the body. Using the micro-scale patterning abilities of the μSLA, bio-bots with feature sizes ten-fold smaller than capable with the existing SLA can be fabricated. Features that allow for incorporation of multiple cell types can be patterned into the hydrogel structure as well. For example, bio-bots that incorporate neurons, as shall be discussed in the following section, will require long channels of small diameter through which the axons can be guided to the engineered muscle strip. Furthermore, bio-bots that must function in diverse and non-ideal environments will require microfabricated soft hydrogel exoskeletons that insulate the bio-bot and provide them with a supply of nutrients. These and other fabrication challenges can only be rendered possible by the precision patterning capabilities of the μSLA.

5.1.3 CONCLUSION

Digital mask based projection stereolithography offers many advantages over currently existing techniques for patterning cells and cell signals in 3D. The μSLA system illustrated in this thesis has the ability to fabricate biocompatible structures with feature sizes that enable a wide array of applications including studies of cell mechanics, programmable tissue engineering, and the development of biological machines and promises to be an indispensible enabling tool in the field of bionanotechnology in the coming years.

5.2 MICROFABRICATED BIOLOGICAL MACHINES

Forward-engineered biological machines and systems with the ability to dynamically sense, process, and respond to external cues define a promising new era of soft robotics. The most intuitive demonstration of controllable behavior is stimulation-induced actuation and locomotion. In this study, biological machines microfabricated via stereolithography served as a platform for the force generation and contractile behavior of engineered skeletal and cardiac muscle. Electrical signals were used to pace and drive contraction of this engineered muscle in the first stage of the study, followed by the more precise noninvasive technique of optical signaling enabled by the emerging field of optogenetics.

5.2.1 FURTHER DEVELOPMENTS IN OPTOGENETIC STIMULATION

In this study, the light-gated Channelrhodopsin-2 ion channel was used to stimulate contraction of engineered muscle in response to blue light of 490 nm wavelength. In muscle tissue that does not demonstrate spontaneous/autonomous contraction, this light-gated channel is sufficient to drive control of the biological machines. However, in muscle tissue that does demonstrate significant autonomous contractile forces, such as those observed in cardiac muscle tissue, a light-activated anion channel that can suppress these action potentials is required. The next step in engineering optogenetically controlled machine with start/stop control is thus the incorporation of the light gated anion channel, halorhodopsin (NpHR), into muscle culture systems via transfection. This anion channel is activated by yellow light of 590 nm wavelength and, in tandem with the blue light activated ChR2 ion channel, can be used to trigger and suppress action potentials in engineered muscle tissue, as required, with high spatiotemporal resolution.

Currently, an LED connected to a function generator is the source of optical stimulation used to drive locomotion of the bio-bots. While this method is functional, it does not take advantage of the high specificity and spatiotemporal resolution enabled by the field of optogenetics. The advantage of this genetic modification technique is that it can be used to excite and pace single muscle cells or portions or whole areas of 2D sheets or 3D strips of engineered muscle. To harness these high-resolution capabilities of optogenetic muscle systems, a new optical stimulation setup has been built (Figure 5.2). In this setup, a customized script tracks bio-

bots using a camera using automated tracking software[§]. A projector and lens system is used to project blue or yellow light onto portions or whole areas of the bio-bot, and the stimulus follows the bio-bot via during locomotion via the automated tracking system. This novel and sophisticated stimulation apparatus allows for precise and dynamic stimulation of engineered muscle systems, allowing for the creation of more intricate bio-bot designs and locomotion mechanisms in the future.

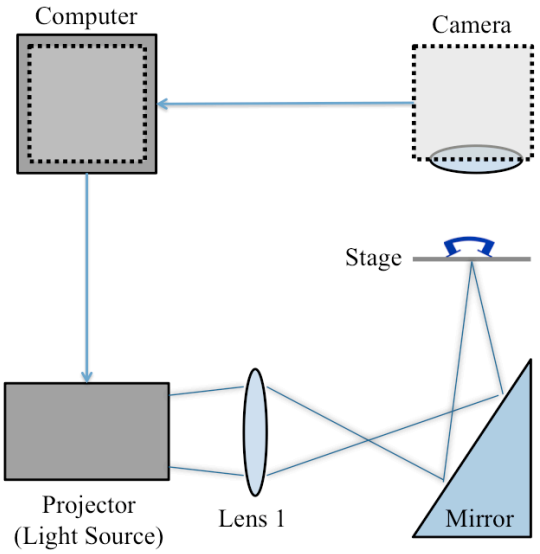

Figure 5.2: Schematic of apparatus to automatically track and stimulate optogenetic bio-bots

5.2.2 BIOLOGICAL CHARACTERIZATION OF ENGINEERED MUSCLE

The bio-bots used in this study have primarily been analyzed from a mechanical perspective in this document, but biological analysis of bio-bots is a significant ongoing challenge in this field. Histology and immunostaining of skeletal muscle based bio-bots have revealed that cells tend to accumulate near the outer periphery of the tissue, within the diffusion distance of 150 μm, as reported in many tissue engineered systems (Novosel 2011). Studies of this kind have led to qualitative understandings of the morphological organization of engineered tissue. For example, staining of the bio-bot muscle strips analyzed in this study has shown that myotubes tend to align in the direction of uniaxial tension imposed by the hydrogel structure and more myotubes are observed in bio-bots supplemented with IGF-1.

§ Custom tracking script was written by Michael Grigola, from Professor Jimmy Hsia's research group, in collaboration with Brian Williams, from Professor Taher Saif's research group at the University of Illinois at Urbana-Champaign.

A next step in the characterization of these muscle strips is calcium staining of muscle strips during contraction. Calcium staining involves staining the muscle tissue with a voltage sensitive dye that fluoresces in response to the calcium ion flow that occurs during an action potential. This will allow for precise visualization of action potential propagation across the engineered muscle tissue, enabling understanding of the force generation and distribution in the macro-scale tissue and motivating newer and more efficient designs (Herron 2012).

5.2.3 INTEGRATION OF MULTIPLE CELL TYPES

Bio-bots capable of controlled actuation and locomotion are but the first step in engineering biological machines. The goal of these technologies is to create truly integrated systems composed of multiple cell types that interact with each other to perform complex sensing, processing, and actuation tasks. Following the experiments in which bio-bot mobility is controlled via external optical signals, the system detailed in this study will start to incorporate optogenetic neurons that interface with the engineered muscle via functional neuromuscular junctions. These neurons will be used to initiate action potentials in the engineered muscle that will drive contractility, force generation, and ultimate actuation of the biological machines. While direct optical stimulation of skeletal muscle as accomplished in the initial experiments will provide “on” or “off” control of bio-bots, these integrated cellular systems containing neuronal networks interfacing with muscle will enable more complex behavior by processing compound signals through neuronal circuits to generate a variety of responses. Eventually, the incorporation of endothelial cells into these biological systems will enable the vascularization of large bio-bots, allowing for better distribution of cells, cell signals, and nutrients throughout the engineered tissue. This is anticipated to lead to more efficient force production in the long term.

The mammalian cell based bio-bots engineered in this study function best in the specific biochemical and physical environment of culture medium maintained at body temperature, 37ºC. In order for bio-bots to be utilized in a variety of applications, they must be robust and capable of functioning in diverse and non-ideal environments. A future direction in engineering such robust biological machines is the incorporation of microfabricated soft synthetic exoskeletons into the bio-bot designs that will provide the machines with insulation and a temporary supply of nutrients. This will dramatically increase the ability of bio-bots to be tailored to a myriad array of sensing and actuation applications.

5.2.4 CONCLUSION

Forward engineered biological systems have many practical applications and can lead to a quantitative understanding of the way integrated cellular systems sense and respond to signals in their environment. The skeletal and cardiac muscle based controllable bioactuators presented in this thesis represent the first step towards engineering biological machines capable of complex functional behaviors.

5.3 A NEW ERA OF DESIGN AND MANUFACTURING

The burgeoning field of additive manufacturing, or "3D printing", centers on the idea of creating three-dimensional objects from digital models. While conventional manufacturing approaches rely on modifying a base material via subtractive processes such as drilling or cutting, 3D printing creates three-dimensional objects through successive deposition of two-dimensional layers. By enabling rapid fabrication of complex objects, 3D printing is revolutionizing the way we think about design and manufacturing.

In stereolithography, a subtype of 3D printing, photopolymers (polymers that change their properties in response to light) are patterned or "cured" into three-dimensional designs through exposure to ultraviolet light. Conventionally, laser-based stereolithography apparatus have used visible or ultraviolet light lasers to trace 2D cross-sections of 3D designs, building complex structures layer by layer from the bottom up. More recently, projection-based stereolithography apparatus have demonstrated the ability to project high resolution 2D light patterns onto photopolymers, allowing for rapid fabrication of complex structures with reduced feature sizes.

Many researchers have explored the use of laser-based stereolithographic microfabrication technologies as a method of printing living cells dispersed in highly absorbent hydrogel polymer matrix. This thesis details the development of a projection-based stereolithography apparatus capable of patterning cells and cell signals at high resolution *in vitro*. This novel enabling technology can be used to create model cellular systems that lead to a quantitative understanding of the way cells sense, process, and respond to signals in their environment.

The emerging field of tissue engineering promises to revolutionize modern medicine by providing an alternative to tissue and organ transplantation through the creation of *in vitro* model

systems that can replicate the structure and function of native tissue. While the goal of "reverse engineering" native tissue is promising for medical applications, this idea of building with biology concurrently brings about a new field: "forward engineering" of biological machines and systems. In addition to rebuilding existing systems with cells, researchers can also design and forward engineer novel systems that harness the innate dynamic abilities of cells to self-organize, self-heal, and self-replicate in response to environmental cues. These machines, which can sense, process, and respond to signals in a dynamic environment, have a myriad array of applications including toxin neutralization and high throughput drug testing *in vitro* and drug delivery and programmable tissue engineered implants *in vivo*.

Throughout history, humans have designed and built machines and systems using "traditional" engineering materials such as wood, metals, and plastics through subtractive manufacturing techniques. The advent of 3D printing additive manufacturing technologies has ushered in a new age of design in which increased complexity of structures and reduced material waste is enabled. Concurrently, the idea of "building with biology", or using cells and instructive biomaterials as building blocks for constructing complex biological substitutes for native tissue, has garnered much momentum. A synthesis of these two fields brings about a new era of technological innovation: using microfabrication technologies to forward engineer biological machines and systems capable of complex functional behavior. By introducing a new set of "building blocks" into the engineer's toolbox, this new era of design and manufacturing promises to open up a field of research that will redefine our world.

REFERENCES

Akiyama, Y., Funakoshi, K., & Morishima, K. (2013). In-air operable biohybrid micromanipulator powered by insect heart muscle tissue (Vol. 1).

Andersson, H., & van den Berg, A. (2004). Microfabrication and microfluidics for tissue engineering: state of the art and future opportunities. *Lab on a Chip*, *4*(2), 98–103.

Anseth, K. S., Bowman, C. N., & Brannon-Peppas, L. (1996). Mechanical properties of hydrogels and their experimental determination. *Biomaterials*, *17*(17), 1647–57.

Arcaute, K., Mann, B. K., & Wicker, R. B. (2006). Stereolithography of three-dimensional bioactive poly(ethylene glycol) constructs with encapsulated cells. *Annals of Biomedical Engineering*, *34*(9), 1429–41.

Bajaj, P., Reddy, B., Millet, L., Wei, C., Zorlutuna, P., Bao, G., & Bashir, R. (2011). Patterning the differentiation of C2C12 skeletal myoblasts. *Integrative Biology*, *3*(9), 897–909.

Bajaj, P., Marchwiany, D., Duarte, C., & Bashir, R. (2012). Patterned Three-Dimensional Encapsulation of Embryonic Stem Cells using Dielectrophoresis and Stereolithography. *Advanced Healthcare Materials*.

Bartolo, P. J. (2011). Stereolithographic Processes. In P. J. Bártolo (Ed.), *Stereolithography: Materials, Processes and Applications* (pp. 1–36). Boston, MA: Springer US.

Bershteyn, M., & Kriegstein, A. R. (2013). Cerebral Organoids in a Dish: Progress and Prospects. *Cell*, *155*(1), 19–20.

Bian, W., & Bursac, N. (2009). Engineered skeletal muscle tissue networks with controllable architecture. *Biomaterials*, *30*(7), 1401–12.

Boland, T., Xu, T., Damon, B., & Cui, X. (2006). Application of inkjet printing to tissue engineering. *Biotechnology Journal*, *1*(9), 910–7.

Boudou, T., Legant, W. R., Mu, A., Borochin, M. A., Thavandiran, N., Radisic, M., … Chen, C. S. (2012). A Microfabricated Platform to Measure and Manipulate the Mechanics of Engineered Cardiac Microtissues. *Tissue Engineering*, *18*, 910–919.

Bryant, S. J., & Anseth, K. S. (2002). Hydrogel properties influence ECM production by chondrocytes photoencapsulated in poly(ethylene glycol) hydrogels. *Journal of biomedical materials research*, *59*(1), 63–72.

Bryant, S. J., Nuttelman, C. R., & Anseth, K. S. (2012). Cytocompatibility of UV and visible light photoinitiating systems on cultured NIH/3T3 fibroblasts in vitro. *Journal of Biomaterials Science Polymer Edition*, *11*(5), 439–457.

Chan, V., Zorlutuna, P., Jeong, J. H., Kong, H., & Bashir, R. (2010). Three-dimensional photopatterning of hydrogels using stereolithography for long-term cell encapsulation. *Lab on a Chip*, *10*(16), 2062–70.

Chan, V., Collens, M. B., Jeong, J. H., Park, K., Kong, H., & Bashir, R. (2012). Directed cell growth and alignment on protein-patterned 3D hydrogels with stereolithography. *Virtual and Physical Prototyping*, *7*(3), 219–228.

Chan, V., Jeong, J. H., Bajaj, P., Collens, M. B., Saif, T. A., Kong, H., & Bashir, R. (2012). Multi-material bio-fabrication of hydrogel cantilevers and actuators with stereolithography. *Lab on a Chip*, *12*(1), 88–98.

Chan, V., Park, K., Collens, M. B., Kong, H., Saif, T. A., & Bashir, R. (2012). Development of miniaturized walking biological machines. *Scientific Reports*, *2*.

Chen, C. S., Mrksich, M., Huang, S., Whitesides, G. M., & Ingber, D. E. (1997). Geometric Control of Cell Life and Death. *Science*, *276*(5317), 1425–1428.

Chiou, P. Y., Ohta, A. T., & Wu, M. C. (2005). Massively parallel manipulation of single cells and microparticles using optical images. *Nature*, *436*(7049), 370–2.

Choi, J.-W., MacDonald, E., & Wicker, R. (2009). Multi-material microstereolithography. *The International Journal of Advanced Manufacturing Technology*, *49*(5-8), 543–551.

Cohen, D. L., Malone, E., Lipson, H., & Bonassar, L. J. (2006). Direct freeform fabrication of seeded hydrogels in arbitrary geometries. *Tissue engineering*, *12*(5), 1325–35.

Cukierman, E., Pankov, R., & Yamada, K. M. (2002). Cell interactions with three-dimensional matrices. *Current Opinion in Cell Biology*, *14*, 633–639.

Deisseroth, K. (2011). Optogenetics. *Nature Met*, *8*(1), 26–29.

Dennis, R. G., & Kosnik, P. E. (2000). Excitability and isometric contractile properties of mammalian skeletal muscle constructs engineered in vitro. *In vitro Cellular & Developmental Biology - Animal*, *36*(5), 327–35.

Du, Y., Lo, E., Ali, S., & Khademhosseini, A. (2008). Directed assembly of cell-laden microgels for fabrication of 3D tissue constructs. *Proceedings of the National Academy of Sciences of the United States of America*, *105*(28), 9522–7.

Engler, A. J., Sen, S., Sweeney, H. L., & Discher, D. E. (2006). Matrix elasticity directs stem cell lineage specification. *Cell*, *126*(4), 677–89.

Fairbanks, B. D., Schwartz, M. P., Bowman, C. N., & Anseth, K. S. (2009). Photoinitiated polymerization of PEG-diacrylate with lithium phenyl-2,4,6-trimethylbenzoylphosphinate: polymerization rate and cytocompatibility. *Biomaterials*, *30*(35), 6702–7.

Fan, C. Y., Tung, Y.-C., Takayama, S., Meyhöfer, E., & Kurabayashi, K. (2008). Electrically Programmable Surfaces for Configurable Patterning of Cells. *Advanced Materials*, *20*(8), 1418–1423.

Fraley, S. I., Feng, Y., Krishnamurthy, R., Kim, D.-H., Celedon, A., Longmore, G. D., & Wirtz, D. (2010). A distinctive role for focal adhesion proteins in three-dimensional cell motility. *Nature cell biology*, *12*(6), 598–604.

Fujita, H., Nedachi, T., & Kanzaki, M. (2007). Accelerated de novo sarcomere assembly by electric pulse stimulation in C2C12 myotubes. *Experimental Cell Research*, *313*(9), 1853–65.

Gaebel, R., Ma, N., Liu, J., Guan, J., Koch, L., Klopsch, C., … Steinhoff, G. (2011). Patterning human stem cells and endothelial cells with laser printing for cardiac regeneration. *Biomaterials*, *32*(35), 9218–30.

Gauvin, R., Chen, Y.-C., Lee, J. W., Soman, P., Zorlutuna, P., Nichol, J. W., … Khademhosseini, A. (2012). Microfabrication of complex porous tissue engineering scaffolds using 3D projection stereolithography. *Biomaterials*, *33*(15), 3824–34.

Griffith, L. G., & Naughton, G. (2002). Tissue engineering--current challenges and expanding opportunities. *Science (New York, N.Y.)*, *295*(5557), 1009–14.

Grogan, S. P., Chung, P. H., Soman, P., Chen, P., Lotz, M. K., Chen, S., & D'Lima, D. D. (2013). Digital micromirror device projection printing system for meniscus tissue engineering. *Acta Biomaterialia*, *9*(7), 7218–26.

Herron, T. J., Lee, P., & Jalife, J. (2012). Optical imaging of voltage and calcium in cardiac cells & tissues. *Circulation Research*, *110*(4), 609–23.

Hinds, S., Bian, W., Dennis, R. G., & Bursac, N. (2011). The role of extracellular matrix composition in structure and function of bioengineered skeletal muscle. *Biomaterials*, *32*(14), 3575–83.

Hinkley, J. A., Morgret, L. D., & Gehrke, S. H. (2004). Tensile properties of two responsive hydrogels. *Polymer*, *45*(26), 8837–8843.

Huang, Y.-C., Dennis, R. G., Larkin, L., & Baar, K. (2005). Rapid formation of functional muscle in vitro using fibrin gels. *Journal of Applied Physiology*, *98*(2), 706–13.

Huh, D., Matthews, B. D., Mammoto, A., Montoya-Zavala, M., Hsin, H. Y., & Ingber, D. E. (2010). Reconstituting organ-level lung functions on a chip. *Science (New York, N.Y.)*, *328*(5986), 1662–8.

Hynd, M. R., Frampton, J. P., Dowell-Mesfin, N., Turner, J. N., & Shain, W. (2007). Directed cell growth on protein-functionalized hydrogel surfaces. *Journal of Neuroscience Methods*, *162*, 255–263.

Iyer, R. K., Chiu, L. L. Y., Reis, L. a, & Radisic, M. (2011). Engineered cardiac tissues. *Current opinion in Biotechnology*, *22*(5), 706–14.

Jakab, K., Norotte, C., Damon, B., Marga, F., Neagu, A., Besch-Williford, C. L., … Forgacs, G. (2008). Tissue engineering by self-assembly of cells printed into topologically defined structures. *Tissue Engineering*, *14*(3), 413–21.

Jeong, J. H., Chan, V., Cha, C., Zorlutuna, P., Dyck, C., Hsia, K. J., … Kong, H. (2012). "Living" microvascular stamp for patterning of functional neovessels; orchestrated control of matrix property and geometry. *Advanced Materials*, *24*(1), 58–63, 1.

Kamm, R. D., & Bashir, R. (2013). Creating Living Cellular Machines. *Annals of Biomedical Engineering*.

Khademhosseini, A., Langer, R., Borenstein, J., & Vacanti, J. P. (2006). Microscale technologies for tissue engineering and biology. *Proceedings of the National Academy of Sciences of the United States of America*, *103*(8), 2480–2487.

Kharaziha, M., Nikkhah, M., Shin, S.-R., Annabi, N., Masoumi, N., Gaharwar, A. K., … Khademhosseini, A. (2013). PGS:Gelatin nanofibrous scaffolds with tunable mechanical and structural properties for engineering cardiac tissues. *Biomaterials*, *34*(27), 6355–6366.

Khodabukus, A., & Baar, K. (2009). Regulating Fibrinolysis to Engineer Skeletal Muscle from the C2C12 Cell Line. *Tissue Engineering*, *15*(3), 501–511.

Kloxin, A. M., Kloxin, C. J., Bowman, C. N., & Anseth, K. S. (2010). Mechanical properties of cellularly responsive hydrogels and their experimental determination. *Advanced Materials*, *22*(31), 3484–94.

Koike, N., Fukumura, D., Gralla, O., Au, P., Schechner, J. S., & Jain, R. K. (1999). Creation of long-lasting blood vessels. *Nature*, *428*, 138–139.

Laakso, J. M., Lewis, J. H., Shuman, H., & Ostap, E. M. (2008). Myosin I can act as a molecular force sensor. *Science*, *321*(5885), 133–6.

Lam, M. T., Huang, Y.-C., Birla, R. K., & Takayama, S. (2009). Microfeature guided skeletal muscle tissue engineering for highly organized 3-dimensional free-standing constructs. *Biomaterials*, *30*(6), 1150–5.

Legant, W. R., Pathak, A., Yang, M. T., Deshpande, V. S., McMeeking, R. M., & Chen, C. S. (2009). Microfabricated tissue gauges to measure and manipulate forces from 3D microtissues. *Proceedings of the National Academy of Sciences of the United States of America*, *106*(25), 10097–10102.

Lin, H., Zhang, D., Alexander, P. G., Yang, G., Tan, J., Cheng, A. W.-M., & Tuan, R. S. (2013). Application of visible light-based projection stereolithography for live cell-scaffold fabrication with designed architecture. *Biomaterials*, *34*(2), 331–9.

Linnenberger, A., Bodine, M. I., Fiedler, C., Roberts, J. J., Skaalure, S. C., Quinn, J. P., … McLeod, R. R. (2013). Three dimensional live cell lithography. *Optics Express*, *21*(8), 10269–10277.

Magdanz, V., Sanchez, S., & Schmidt, O. G. (2013). Development of a Sperm-Flagella Driven Micro-Bio-Robot. *Advanced Materials*.

Martel, S., Tremblay, C. C., Ngakeng, S., & Langlois, G. (2006). Controlled manipulation and actuation of micro-objects with magnetotactic bacteria. *Applied Physics Letters*, *89*(23), 89–91.

Matsumoto, T., Sasaki, J., Alsberg, E., Egusa, H., Yatani, H., & Sohmura, T. (2007). Three-Dimensional Cell and Tissue Patterning in a Strained Fibrin Gel System. *PLoS One*, (11).

McSpadden, L. C., Kirkton, R. D., & Bursac, N. (2009). Electrotonic loading of anisotropic cardiac monolayers by unexcitable cells depends on connexin type and expression level, 339–351.

Melchels, F. P. W., Feijen, J., & Grijpma, D. W. (2010). A review on stereolithography and its applications in biomedical engineering. *Biomaterials*, *31*(24), 6121–30.

Miller, J. S., Stevens, K. R., Yang, M. T., Baker, B. M., Nguyen, D.-H. T., Cohen, D. M., … Chen, C. S. (2012). Rapid casting of patterned vascular networks for perfusable engineered three-dimensional tissues. *Nature Materials*, *11*(9), 768–74.

Mironov, V., Prestwich, G., & Forgacs, G. (2007). Bioprinting living structures. *Journal of Materials Chemistry*, *17*(20), 2054–2060.

Mirsaidov, U., Scrimgeour, J., Timp, W., Beck, K., Mir, M., Matsudaira, P., & Timp, G. (2008). Live cell lithography: using optical tweezers to create synthetic tissue. *Lab on a Chip*, *8*(12), 2174–81.

Morimoto, Y., Kato-Negishi, M., Onoe, H., & Takeuchi, S. (2013). Three-dimensional neuron-muscle constructs with neuromuscular junctions. *Biomaterials*.

Nawroth, J. C., Lee, H., Feinberg, A. W., Ripplinger, C. M., McCain, M. L., Grosberg, A., … Parker, K. K. (2012). A tissue-engineered jellyfish with biomimetic propulsion. *Nature Biotechnology*, *30*(8), 792–7.

Neal, D., Sakar, M. S., & Asada, H. H. (2013). Optogenetic Control of Live Skeletal Muscles : Non-Invasive , Wireless , and Precise Activation of Muscle Tissues. In *American Control Conference* (pp. 1513–1518).

Norotte, C., Marga, F. S., Niklason, L. E., & Forgacs, G. (2009). Scaffold-free vascular tissue engineering using bioprinting. *Biomaterials*, *30*(30), 5910–7.

Novosel, E. C., Kleinhans, C., & Kluger, P. J. (2011). Vascularization is the key challenge in tissue engineering. *Advanced drug delivery reviews*, *63*(4-5), 300–11.

Ott, H. C., Matthiesen, T. S., Goh, S.-K., Black, L. D., Kren, S. M., Netoff, T. I., & Taylor, D. a. (2008). Perfusion-decellularized matrix: using nature's platform to engineer a bioartificial heart. *Nature Medicine*, *14*(2), 213–21.

Ovsianikov, A., Gruene, M., Pflaum, M., Koch, L., Maiorana, F., Wilhelmi, M., … Chichkov, B. (2010). Laser printing of cells into 3D scaffolds. *Biofabrication*, *2*(1).

Pampaloni, F., Reynaud, E. G., & Stelzer, E. H. K. (2007). The third dimension bridges the gap between cell culture and live tissue. *Nature Reviews*, *8*(10), 839–45.

Park, H., Cannizzaro, C., Vunjak-Novakovic, G., Langer, R., Vacanti, C. A., & Farokhzad, O. C. (2007). Nanofabrication and microfabrication of functional materials for tissue engineering. *Tissue Engineering*, *13*(8), 1867–77.

Peppas, N. A., Hilt, J. Z., Khademhosseini, A., & Langer, R. (2006). Hydrogels in Biology and Medicine: From Molecular Principles to Bionanotechnology. *Advanced Materials*, *18*(11), 1345–1360.

Petersen, O. W., Rønnov-Jessen, L., Howlett, a R., & Bissell, M. J. (1992). Interaction with basement membrane serves to rapidly distinguish growth and differentiation pattern of normal and malignant human breast epithelial cells. *Proceedings of the National Academy of Sciences of the United States of America*, *89*(19), 9064–8.

Powell, C. a, Smiley, B. L., Mills, J., & Vandenburgh, H. H. (2002). Mechanical stimulation improves tissue-engineered human skeletal muscle. *American journal of physiology. Cell physiology*, *283*(5), C1557–65.

Radisic, M., Park, H., Shing, H., Consi, T., Schoen, F. J., Langer, R., … Vunjak-Novakovic, G. (2004). Functional assembly of engineered myocardium by electrical stimulation of cardiac myocytes cultured on scaffolds. *Proceedings of the National Academy of Sciences of the United States of America*, *101*(52), 18129–34.

Sakar, M. S., Neal, D., Boudou, T., Borochin, M. A., Li, Y., Weiss, R., … Asada, H. H. (2012). Formation and optogenetic control of engineered 3D skeletal muscle bioactuators. *Lab on a Chip*, *12*(23), 4976–85.

Sawkins, M. J., Shakesheff, K. M., Bonassar, L. J., & Kirkham, G. R. (2013). 3D Cell and Scaffold Patterning Strategies in Tissue Engineering. *Recent Patents on Biomedical Engineering*, *6*, 3–21.

Shin, S. R., Jung, S. M., Zalabany, M., Kim, K., Zorlutuna, P., Kim, S. bok, … Khademhosseini, A. (2013). Hydrogel Sheets for Engineering Cardiac Constructs and Bioactuators. *ACS Nano*.

Simmel, F., & Yurke, B. (2001). Using DNA to construct and power a nanoactuator. *Physical Review E*, *63*(4), 63–67.

Soman, P., Chung, P. H., Zhang, A., & Chen, S. (2013). Digital microfabrication of user-defined 3D microstructures in cell-laden hydrogels. *Biotechnology and Bioengineering*.

Song, J. J., Guyette, J. P., Gilpin, S. E., Gonzalez, G., Vacanti, J. P., & Ott, H. C. (2013). Regeneration and experimental orthotopic transplantation of a bioengineered kidney. *Nature Medicine*.

Souza, G. R., Molina, J. R., Raphael, R. M., Ozawa, M. G., Stark, D. J., Levin, C. S., … Pasqualini, R. (2010). Three-dimensional tissue culture based on magnetic cell levitation. *Nature Nanotechnology*, *5*(4), 291–6.

Stampfl, J., & Liska, R. (2011). Polymerizable Hydrogels for Rapid Prototyping: Chemistry, Photolithography, and Mechanical Properties. In P. J. Bártolo (Ed.), *Stereolithography: Materials, Processes and Applications*. Boston, MA: Springer US.

Stephens-Altus, J. S., Sundelacruz, P., Rowland, M. L., & West, J. L. (2011). Development of bioactive photocrosslinkable fibrous hydrogels. *Journal of Biomedical Materials Research*, *98*(2), 167–76.

Sun, C., Fang, N. X., Wu, D. M., & Zhang, X. (2005). Projection micro-stereolithography using digital micro-mirror dynamic mask. *Sensors and Actuators*, *121*(1), 113–120.

Thavandiran, N., Dubois, N., Mikryukov, A., Massé, S., Beca, B., Simmons, C. a, … Zandstra, P. W. (2013). Design and formulation of functional pluripotent stem cell-derived cardiac microtissues. *Proceedings of the National Academy of Sciences of the United States of America*, 1–10.

Théry, M. (2010). Micropatterning as a tool to decipher cell morphogenesis and functions. *Journal of Cell Science*, *123*(24), 4201–13.

Tibbitt, M. W., & Anseth, K. S. (2009). Hydrogels as extracellular matrix mimics for 3D cell culture. *Biotechnology and Bioengineering*, *103*(4), 655–63.

Tsang, V. L., Chen, A. A., Cho, L. M., Jadin, K. D., Sah, R. L., DeLong, S., … Bhatia, S. N. (2007). Fabrication of 3D hepatic tissues by additive photopatterning of cellular hydrogels. *FASEB journal : official publication of the Federation of American Societies for Experimental Biology*, *21*(3), 790–801.

Vale, R. D., Reese, T. S., & Sheetz, M. P. (1985). Identification of a novel force-generating protein, kinesin, involved in microtubule-based motility. *Cell*, *42*(1), 39–50.

Vunjak-Novakovic, G., Tandon, N., Godier, A., Maidhof, R., Marsano, A., Martens, T. P., & Radisic, M. (2010). Challenges in Cardiac Tissue Engineering. *Tissue Engineering*, *15*(2), 169–187.

Watt, F. M., & Huck, W. T. S. (2013). Role of the extracellular matrix in regulating stem cell fate. *Nature Reviews*, *14*(8), 467–73.

Williams, C. G., Kim, T. K., Taboas, A., Malik, A., Manson, P., & Elisseeff, J. (2003). In Vitro Chondrogenesis of Bone Marrow-Derived Mesenchymal Stem Cells in a Photopolymerizing Hydrogel. *Tissue Engineering*, *9*(4), 679–688.

Williams, C. G., Malik, A. N., Kim, T. K., Manson, P. N., & Elisseeff, J. H. (2005). Variable cytocompatibility of six cell lines with photoinitiators used for polymerizing hydrogels and cell encapsulation. *Biomaterials*, *26*(11), 1211–8.

Xia, C., & Fang, N. X. (2009). Fully three-dimensional microfabrication with a grayscale polymeric self-sacrificial structure. *Journal of Micromechanics and Microengineering*, *19*(11).

Yeh, J., Ling, Y., Karp, J. M., Gantz, J., Chandawarkar, A., Eng, G., … Khademhosseini, A. (2006). Micromolding of shape-controlled, harvestable cell-laden hydrogels. *Biomaterials*, *27*(31), 5391–8.

Yurke, B., Turber, A. J., Jr, A. P. M., Simmel, F. C., & Neumann, J. L. (2000). A DNA-fuelled molecular machine made of DNA. *Nature*, *406*, 605–608.

Zhang, H., Hutmacher, D. W., Chollet, F., Poo, A. N., & Burdet, E. (2005). Microrobotics and MEMS-based fabrication techniques for scaffold-based tissue engineering. *Macromolecular Bioscience*, *5*(6), 477–89.

Zhang, A. P., Qu, X., Soman, P., Hribar, K. C., Lee, J. W., Chen, S., & He, S. (2012). Rapid fabrication of complex 3D extracellular microenvironments by dynamic optical projection stereolithography. *Advanced Materials*, *24*(31), 4266–70.

Zimmermann, W.-H., Melnychenko, I., Wasmeier, G., Didié, M., Naito, H., Nixdorff, U., … Eschenhagen, T. (2006). Engineered heart tissue grafts improve systolic and diastolic function in infarcted rat hearts. *Nature Medicine*, *12*(4), 452–8.

Zorlutuna, P., Jeong, J. H., Kong, H., & Bashir, R. (2011). Stereolithography-Based Hydrogel Microenvironments to Examine Cellular Interactions. *Advanced Functional Materials*, *21*(19), 3642–3651.